Convair Aerospace Report CASD-NAS-73-011

CRACK GROWTH BEHAVIOR OF 2219-T87 ALUMINUM ALLOY FROM 20° K (-423° F) TO 422° K (300° F)

Prepared for
National Aeronautics and Space Administration
Lyndon B. Johnson Space Center
Contract NAS9-12445

GENERAL DYNAMICS
Convair Aerospace Division

Convair Aerospace Report CASD-NAS-73-011

CRACK GROWTH BEHAVIOR OF 2219-T87 ALUMINUM ALLOY FROM 20° K (-423° F) TO 422° K (300° F)

W. E. Witzell

August 1973

Prepared for
National Aeronautics and Space Administration
Lyndon B. Johnson Space Center
Contract NAS9-12445

Prepared by
CONVAIR AEROSPACE DIVISION OF GENERAL DYNAMICS
San Diego, California

Page Intentionally Left Blank

FOREWORD

The aluminum alloy 2219-T87 has great potential for use as a cryogenic material for various manned and unmanned aerospace vehicles. Although its properties are generally known, toughness characteristics in various grain directions when the material is machined from thick plates and subjected to various environments have not been documented. This program, sponsored by the NASA Johnson Space Center, was designed to determine these properties between 20°K (-423°F) and 423°K (300°F).

Initially, the program was under the direction of S. V. Glorioso of the NASA-JSC, but the bulk of the study was directed by J. W. Smith of that agency. Both of these gentlemen contributed generously to this program, as did R. G. Forman, also of NASA-JSC.

A number of personnel at General Dynamics Convair Aerospace participated in the program including Mr. C. J. Kropp, who was involved in testing, data reduction, and fractography.

Page Intentionally Left Blank

TABLE OF CONTENTS

TABLE OF CONTENTS, Contd

LIST OF ILLUSTRATIONS

LIST OF TABLES

LIST OF TABLES, Contd

SECTION 1

INTRODUCTION

The use of 2219-T87 aluminum alloy has been proposed as a tank material candidate for virtually every version of the space shuttle. Characteristics of the material that make it an attractive candidate include good strength-to-weight ratio, good weldability, and adequate cryogenic properties. Some data indicates that the material has good toughness and resistance to stress corrosion cracking. However, data is not available over the full range of thicknesses expected in service. Since toughness is dependent on thickness, this becomes of great importance.

In addition, various versions of aerospace vehicles use some sort of integrally stiffened structure in the biaxially loaded tank walls. Such configurations must be machined from rather thick plate to account for the stiffener height, but must also be used as the relatively thin tank wall. There has been much discussion but little substantiating data as to whether the toughness of a 1/8-inch-thick material, for instance, is equivalent to that of the same material thickness machined from a rather thick plate; e.g., 3 inches (7.6 cm). Also in dispute is the variation of toughness through the thickness of the plate. Because of machining costs, it is assumed that the tank wall itself will be located at the outer portion of the thick plate. However, it is prudent to determine if that location has adequate toughness or whether it is more advantageous to remove the outer skin.

Also important is the possibility that differences in grain direction may influence toughness or flaw growth characteristics of the alloy when a rather thick plate is used as a base material. When there is a short transverse property problem, however, it is generally the result of rolling and consequently is more likely to occur in thinner materials. Unfortunately, the effect is much more difficult to measure in thinner materials by tensile and toughness specimen tests.

Advanced aerospace programs require rather long lifetimes for the vehicles involving a variety of environments, temperatures, and exposure times. A hydrogen tank, for example, must perform with liquid hydrogen inside even though cryogenic insulation may keep the tank wall to temperatures well above 20°K (-423°F), be exposed to exterior temperatures up to 422°K (300°F), and remain at rest in a sea coast atmosphere for a relatively long time. Any or all of these conditions could have an effect on the fracture characteristics of the 2219-T87 alloy.

Even if all types of fracture characteristics in different environments were known, many of the details of crack behavior in complicated stress fields would not be predictable. Flaw growth characteristics of materials in the form of structural shapes

commonly used in aerospace vehicles are quite complicated. Some attempts to examine flaw growth from holes and weld land areas have been made, but prediction methods have not been verified. Despite this paucity of data, the problem of cracks growing from loaded holes does exist, as evidenced by some well publicized fractures of military airplane components.

During 1971, NASA MSC became interested in the behavior of 2219-T87 aluminum for use in space shuttle tankage. One problem area with this material was noted, however: the low yield strength and lower toughness common in the weldments. To examine this problem, NASA proposed a program to test this material in various welded conditions. Convair Aerospace consequently joined a NASA/industry cooperative program to determine properties of weldments of 2219 as well as several other alloys. Under the Space Shuttle Phase B program, Convair welded a number of thick plates using electron beam, TIG-MIG, and pulsed TIG methods. Initial tests by the NASA showed that improved properties could be obtained from the more sophisticated weld techniques. (Report Number NASA TND-7377.)

Subsequently, NASA MSC awarded the current R&D contract to Convair Aerospace to determine the toughness and flaw growth rates of the same material in the parent metal condition at various temperatures from 20 to 422°K (-423 to 300°F).

1.1 FRACTURE MECHANICS

Eventually, the problem of brittle fracture became refined to a general basic theory. If a crack occurs in a material, and the specimen is subjected to loading causing an increase in stress level, the crack may propagate. If the amount of energy released by cracking exceeds the energy required to crack the material, the crack will be self-propagating at a rapid rate until complete failure occurs.

A brittle material generally has a low threshold of energy release, causing rapid or catastrophic propagation. Many attempts have been made to measure this energy level by such means as the Charpy-V notch impact test or by tensile tests of edge-notched specimens. Although both methods have some utility, the most useful test is the fracture mechanics test. This test required two measurements: 1) maximum gross stress (obtained by observation of the maximum load) and 2) critical crack length.

The stress level around the tip of an advancing crack is governed by the stress intensity factor (K), which is a function of the gross stress in the material and the existing crack length. Under a loading situation when the stress intensity factor reaches the point that it drives the crack to rapid propagation, the resultant K factor is called "critical" and is known as fracture toughness or critical crack intensity factor (K_c).

In fracture toughness testing of engineering materials, it is important to characterize the elastic behavior of the material and to understand the nature of stress and

strain within the body. From elastic theory, stress at any point can be described by six quantities. A condition of plane stress is said to exist in a thin plate loaded by forces at the boundary parallel to the plane of the plate if three of the components are equal to zero (that is, if a normal stress component and its associated shear stresses are zero). These components are considered to be zero everywhere through the thickness. If the plate described is very thick and axial displacement at the ends is prevented, the resulting condition is called plane strain.

If conditions of plane strain exist, a somewhat different approach is used. When the crack begins to advance, the resultant redistribution of stresses may be a mixed mode of plane stress and plane strain. Since measurements or data must be obtained before the transition is made, plane-strain measurements are usually known as "first mode" or "opening mode" characteristics. The problem, then, becomes one of determining the stress, stress intensity factors, and crack length associated with opening mode of cracking. The sudden re-initiation of a crack or notch is occasionally accompanied by an audible noise that has been called "pop-in". Measurement of the stress in a specimen at this point permits determination of a close approximation of the plane-strain fracture toughness. If such a noise is not detected, the critical stress must be obtained by other means.

The ATSM Committee on Fracture Testing suggested that their original suggestions were in error and that more stringent requirements be placed on the thickness of specimens to be used for determining plane-strain fracture toughness (K_{Ic}). They recommend that minimum thickness be determined by:

$$B = \frac{2.5\, K_{Ic}^{2}}{\sigma_{ys}^{2}}$$

where

B = specimen thickness, cm (inches)

K_{Ic} = plane strain fracture toughness, $MN/M^{3/2}$ ($ksi\sqrt{in.}$)

σ_{ys} = yield strength, MN/m^{2} (ksi)

Even more recently, the 2.5 factor has been questioned for materials other than 7075 aluminum alloys tested at room temperature. This factor may be as low as 2.0, but insufficient data is available for verification at this time.

Two ASTM special technical publications (References 1 and 2) provide excellent discussions of plane-strain testing.

Unfortunately, a great deal of the fracture testing performed to date falls in the mixed-mode category and is therefore thickness-dependent. Further, the abundance of test specimen configurations have frequently made the data impossible to compare.

1.2 CYCLIC TESTING

The influence of a flaw in the behavior of a specimen under repeated loading has been known for some time in the general area of fatigue testing. It is common practice to measure fatigue strength or run out of a material specimen that contains a machined notch or hole with a specific stress concentration. In the past decade, however, the measurement of crack growth as a function of the applied stress intensity factor has become prevalent. Cyclic growth rate appears to be a function of the difference in maximum and minimum stress intensity factors for a given cycle. This value (ΔK) is a function of the stress ratio (R) as follows.

$$\Delta K = \sigma_{max} (1-R) f(a)$$

where

σ_{max} = maximum applied stress

R = minimum stress/maximum stress

f (a) = function of crack size

It is customary to plot the crack growth rate da/dN (the crack growth dimension divided by the associated number of cycles) against ΔK using log-log coordinates. These plots become functions of environment, cyclic frequency, material thickness, tempers, etc., and must be used with care.

1.3 SUSTAINED LOAD TESTING

Sustained load testing (sometimes called stress corrosion crack testing) also measures subcritical crack growth. This test was originally devised to determine the threshold below which a given crack would not propagate. Several variations measure the time to failure at a given stress intensity level, time to initial crack growth, and the crack growth per unit of time (da/dt).

In all cases, the applied load is held constant, usually in the presence of an aggressive environment. A common data presentation relates applied stress-intensity factor to the time to cracking or failure.

SECTION 2

TECHNICAL APPROACH

The objectives of this study are to:

a. Evaluate toughness and crack growth characteristics of 2219-T87 aluminum alloy plate under static, cyclic, and sustained load conditions for each principal grain direction.

b. Determine the effect of thickness on the cyclic and sustained load flaw growth rates of 2219 aluminum tested in various environments.

c. Examine crack growth behavior in the 2219 material when the crack originates in a loaded bolt hole.

Only one alloy was examined during this program: 2219 aluminum in the T87 temper. However, the material was obtained in 8.26 cm (3.25 in.) thick plate, which caused special handling problems and special problems in the location documentation of test specimens.

The two plates provided by the NASA were about 8.26 by 228.6 by 254 cm (3.25 by 90 by 100 in.). While property certifications were not available, it was determined that the material was ordered from the mill with the requirement that the mechanical properties be equivalent to the T87 temper of 2219.

In thick plates of this size, there is always the chance that, the required cold work (5 to 7 percent) was not obtained uniformly and the acceptable minimum properties are satisfactory for another temper such as T81 as well as T87.

To expedite specimen fabrication, the two plates were sawed into more manageable pieces shortly after initial inspection and specimen layout. The plates were arbitrarily designated as Plate A and Plate B.

Two drawings were prepared to locate each type of specimen used in this program (Figures 1 and 2). Each fracture specimen carried the location number as part of its individual identification number. For convenience, the face of the plate containing the layout and identification was known as the top and specimens taken from that face carried the designation T.

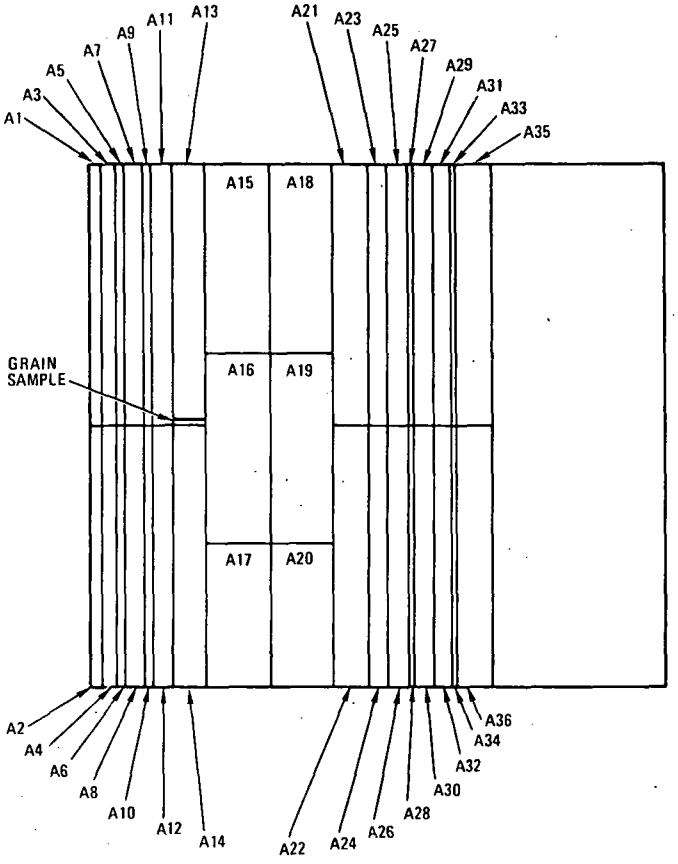

Figure 1. Specimen Location, Plate A

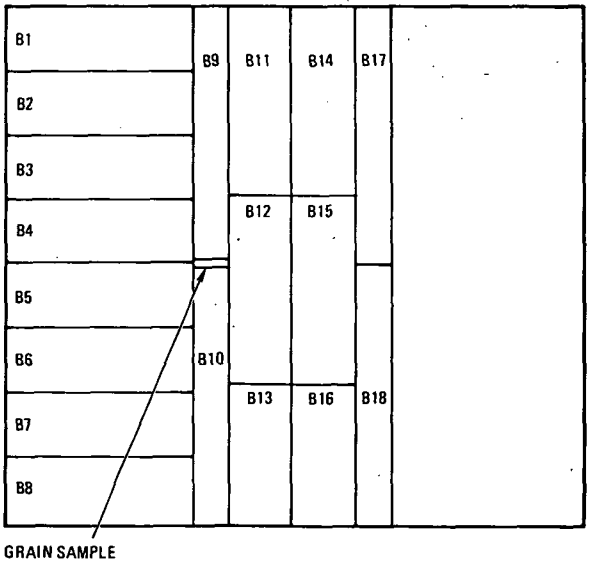

Figure 2. Specimen Location, Plate B

Some typical identifications are:

a. A19-B-LT [0.38 cm (1/8 in.) part through crack specimen]

1. Located in Plate A at location A19.

2. Cut from the bottom of the plate.

3. Direction of loading is parallel to the long-transverse grain direction.

b. A11-ST (3A) - 8 [2.54 cm (1.0 in.) DCB]

1. Located in Plate A at location A11.

2. Loaded in the short transverse direction.

3. Direction of crack growth 3A or in the direction of the longitudinal grain direction (see orientation sketch, Figure 3).

4. The eighth specimen fabricated in this area and of this type.

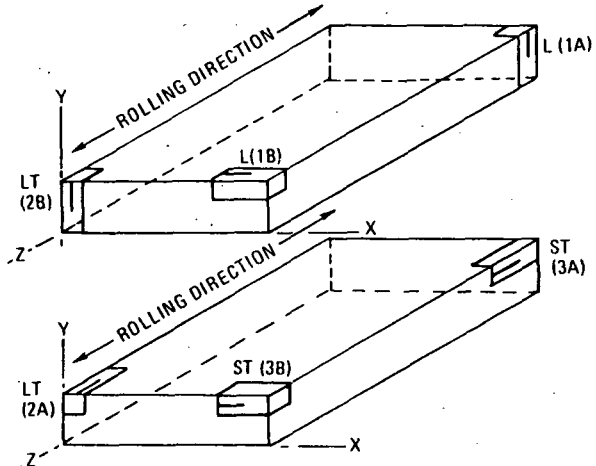

1A LONGITUDINAL SPECIMEN – CRACK IN XY PLANE PROPAGATING IN SHORT TRANSVERSE DIRECTION

1B LONGITUDINAL SPECIMEN – CRACK IN XY PLANE PROPAGATING IN LONG TRANSVERSE DIRECTION

2A LONG TRANSVERSE SPECIMEN – CRACK IN YZ PLANE PROPAGATING IN LONGITUDINAL DIRECTION

2B LONG TRANSVERSE SPECIMEN – CRACK IN YZ PLANE PROPAGATING IN SHORT TRANSVERSE DIRECTION

3A SHORT TRANSVERSE SPECIMEN – CRACK IN XZ PLANE PROPAGATING IN LONGITUDINAL DIRECTION

3B SHORT TRANSVERSE SPECIMEN – CRACK IN XZ PLANE PROPAGATING IN LONG TRANSVERSE DIRECTION

Figure 3. Orientation of DCB and Compact Specimens in Rolled Plate

2.1 MECHANICAL PROPERTIES AND METALLOGRAPHIC EVALUATION

A total of 36 tensile specimens were tested to characterize mechanical properties at various locations in the 8.26 cm (3.25 in.) 2219-T87 aluminum alloy plate. The tensile specimen was excised from one edge of the plates in four locations to represent the center width, each quarter width, and one edge. Longitudinal and long transverse test specimens were excised at T/4 (T = thickness) and machined into standard 12.82 cm (0.505-in.) diameter round tensile specimens with threaded ends. Short transverse tensile specimens were 8.89 cm (0.350-in.) diameter, with subsize specimens proportional to the standard.

Tensile specimens were tested at 422°K (+300°F), ambient, 78°K (-320°F), and 20°K (-423°F) to determine ultimate tensile strength, yield strength at 0.2 percent offset,

elongation, and elastic modulus. Specimens were taken at various locations within the plate thickness and in the vicinity of the tensile specimens for metallographic mounts. The microstructure was examined, and microhardness readings as well as photomicrographs were taken at each location.

All tensile specimens were instrumented with standard extensometers to determine tensile yield strength and modulus of elasticity. Tests were performed in Tinius Olsen test machines. Elevated-temperature tests were performed in a Missimers oven installed in an Instron test machine. Cryogenic test specimens were immersed in liquid nitrogen or liquid hydrogen, instrumented with cryo-extensometers, and tested at normal strain rates in the test machines.

2.2 FRACTURE TEST SPECIMENS AND TECHNIQUES

Two general types of specimens were tested under this program: single-edge notch specimens and surface notch (part-through crack) specimens.

Two types of edge-notched specimens were used. For 0.318 cm (0.125 in.) thick materials, a specimen resembling the ASTM standard (but with a face groove) was used (Figure 4). This specimen was machined with a gage-seating groove at the end of the notch and a cyclindrical hole near the root of the notch to accommodate an environmental chamber. The purpose of the face groove was to encourage the running crack to remain in a plane perpendicular to the direction of applied load.

For testing of 2.54 cm (1.0 in.) thick material, a double cantilever beam was designed, also containing face grooves, gage seats, and environmental chamber holes (Figure 5).

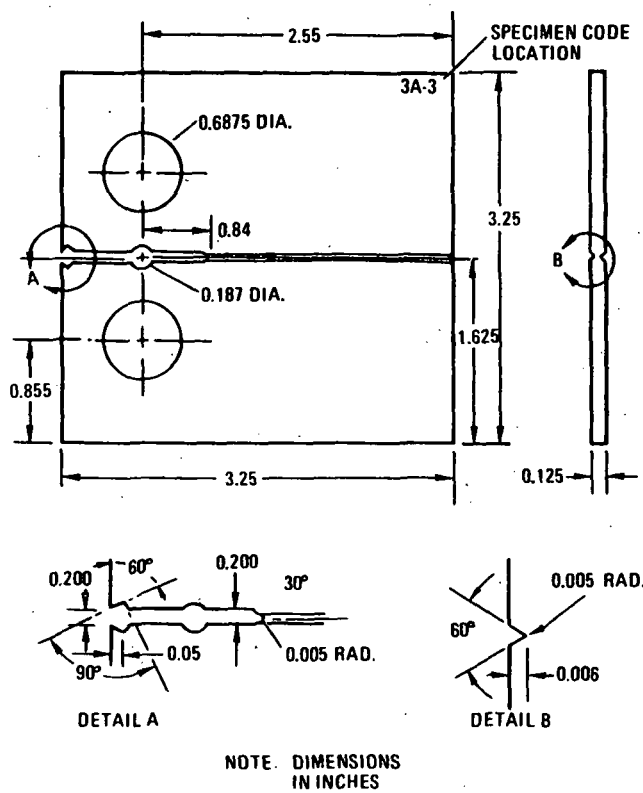

Figure 4. Fracture Test Specimen (0.318 cm)

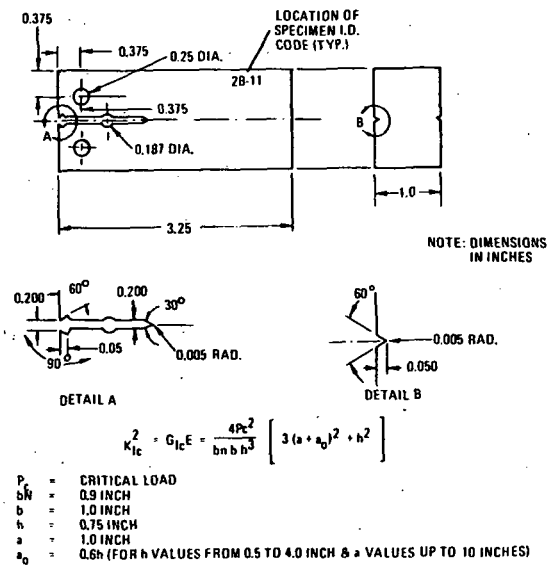

Figure 5. Double Cantilever Beam Specimen (2.54 cm)

2.2.1 EDGE NOTCH FRACTURE TESTS, 2.54 cm (1.0 in.). The uniform (constant height) double cantilever beam (DCB) specimen shown in Figure 5 was chosen over the contoured (tapered) DCB specimens (References 3 and 4) because the uniform type allows a more economical use of the test material. The DCB specimen selected was designed to be tested using external dead loading as opposed to the bolt-loaded constant-deflection test specimen. This approach was used primarily to obtain both threshold values and possible flaw growth rates. (The constant-deflection test is useful in obtaining threshold values, but provides no growth data). Further, the same type of specimen could be used in tensile, fatigue, and sustained load tests.

The slightly greater amount of material consumed per specimen, 2.54 cm (1.0 in.) by 3.81 cm (1.5 in.) compared to 2.54 by 2.54 cm, is considered negligible compared to the increased accuracy of the test data. Pioneer programs conducted by Mostovoy, Crosley, and Ripling (Reference 4), Amateu and Steigerwald (Reference 5), Hoagland (Reference 6), and Hoagland, Bennent, and Howe (Reference 7) substantiate the merits of using uniform DCB specimens loaded by pin grip ends.

The specimen design included side grooves for controlling the direction of crack growth. Experience at Convair Aerospace as well as at other locations (References 4, 7, 9) has shown that side grooves are advantageous not only in controlling crack growth direction but also in the reduction of shear lip formation, which aids in obtaining plain strain fracture.

The DCB specimen included a 0.475 cm (0.187 in.) diameter hole drilled in the notch area for the specimens tested in controlled-humidity air at room temperature and in the aqueous 3.5-percent solution of sodium chloride (Na Cl). Convair Aerospace had conducted crack growth studies in controlled humidity and in Na Cl solution with modified DCB specimens of D6ac steel, and it was felt that the same approach could be used for specimens fabricated from aluminum. A specially designed liquid container was attached to the DCB specimen fabricated from aluminum.

A silicone rubber plug was inserted in the 0.475 cm (0.187 in.) hole. A smaller hole was provided in the plug for a tight fitting machine screw. The liquid container was made of clear plastic to allow observation and crack growth measurements. A rubber O-ring was placed in a groove machined in the plastic container to prevent leakage of the NaCl solution. The plastic containers also contained fill and drain holes so that fresh NaCl solution was in contact with the advancing crack. A constant relative humidity of 52 percent at 293°K (68°F) for crack growth studies was obtained with the same liquid container described above. Glass vials containing a saturated solution of sodium dichromate (plus excess crystals) were carefully placed in the container as shown in Figure 6, and attached to the specimen. Since the volume of air in the container was small and the rubber O-rings and plug provided a tight seal, environmental humidity in the container for room temperature testing was easily controlled. Small fluctuations of temperature in the laboratory have negligible changes in the relative humidity within the attached container.

2.2.2 EDGE NOTCH FRACTURE TESTS

0.318 cm (0.125 in.) MATERIAL. The effect of test specimen thickness was examined by testing 0.318-cm-thick specimens machined from 8.26 cm (3.25 in.) thick plate of 2219-T87 aluminum alloy. Static fracture (K_X), cyclic stress crack growth (da/dN), sustained stress crack growth rates (da/dt), and sustained stress threshold factors (K_{TH}) were determined for 42 test specimens. Twelve specimens were tested at 78°K (-320°F) in liquid nitrogen to determine the critical plane-stress fracture toughness factor (K_X).

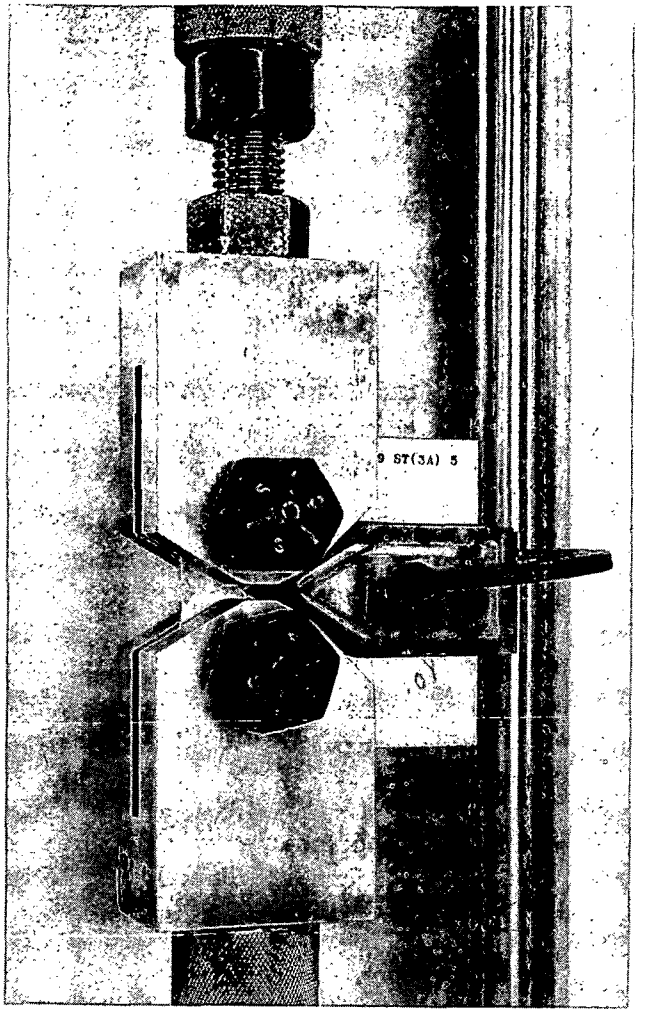

Figure 6. Sustained Load Test of 0.318 cm Fracture Specimen in Environmental Chamber

The compact type of fracture toughness specimen was selected because it offers the most economical use of material and, like the DCB specimen, allowed multiple test data from each specimen. Except for the thickness, the specimen conforms to the compact specimen described in ASTM E399 (Reference 10) and by Wessel (Reference 11). The side grooves were used so that the direction and inclination of the advancing crack could be controlled, even though some investigators question the use of the side grooves (Reference 7). This specimen design also allows the crack length, a, to be varied greatly. Mathematical solutions and compliance data (References 11 and 12) allow the dimensionless crack parameter, a/W, to have a range of 0.3 to 0.8 (with extrapolation to 1.0). The range of a/W in ASTM 399 is much smaller and is limited to a minimum of 0.45 and a maximum of 0.55.

The 0.475 cm (0.187 in.) diameter hole is required for the specimens tested at 50-percent relative humidity at room temperature and in the 3.5-percent aqueous solution of NaCl. The plastic containers used for the DCB specimens were also used for the 0.318 cm (0.125 in.) compact specimens.

Integral knife edges at the mouth of the machined notch were used to attach a displacement gage (Figure 7) for obtaining a record of load versus crack opening displacement. Twelve specimens were tested at 78°K (-320°F) in liquid nitrogen to determine the critical plane stress fracture toughness factor, K_X.

Since one objective of this program was to determine the variation of crack intensity factor with grain orientation, it was necessary to carefully identify all specimens with respect to their grain orientation as mentioned earlier, a master drawing identified the location in each plate of each type of specimen. Two plates were used (identified as A and B) Within the designated area, specimens were cut in three grain directions. For consistency, the grain direction designation also predetermined the direction of loading. In addition to direction of loading, it was necessary to know the direction of intended crack propagation. The orientations and identifications of the six fracture-type specimens are shown in Figure 3. As an example, specimen designation L(1B) means that:

a. This longitudinal specimen is loaded in the longitudinal grain direction.

b. The plane of the crack is that formed by the long transverse and the short transverse grain directions.

c. The intended path of crack propagation is in the long transverse direction.

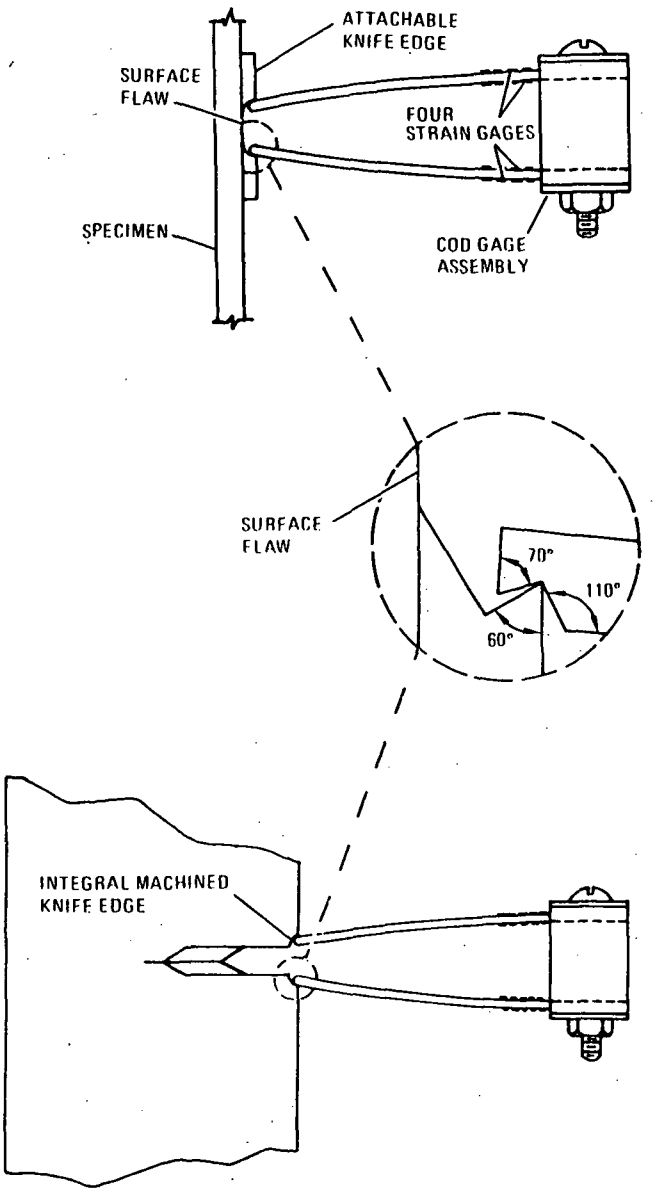

Figure 7. Methods of Installing Crack Opening Displacement Gages

The 0.318 cm (0.125 in.) compact specimens scheduled for this program were:

Type Specimen	K_c LN_2	K_c and Cyclic Growth - RT Air 0.1 Hz	1.0 Hz	10 Hz	K_c and Sustained Stress Growth NaCl Solution
L(1A)	2		2		2
L(1B)	1		1		1
LT(2B)	2		2		2
LT(2A)	1		1		1
ST(3A)	3	3	3	3	3
ST(3B)	3		3		3
Total	12	3	12	3	12

2.2.3 PART-THROUGH CRACK TESTS. A series of 0.318 cm (0.125 in.) and 2.54 cm (1.0 in.) thick part-through crack (PTC) or surface flaw specimens was fabricated from the same 8.26 cm (3.25 in.) thick material used for all other tests. Specimens were oriented only in longitudinal and long transverse grain directions; i.e., the direction of loading of the specimens were in longitudinal and long transverse directions. Unlike other types of specimens, however, crack growth in surface-notched specimens, is in more than one direction in the plane perpendicular to the direction of loading.

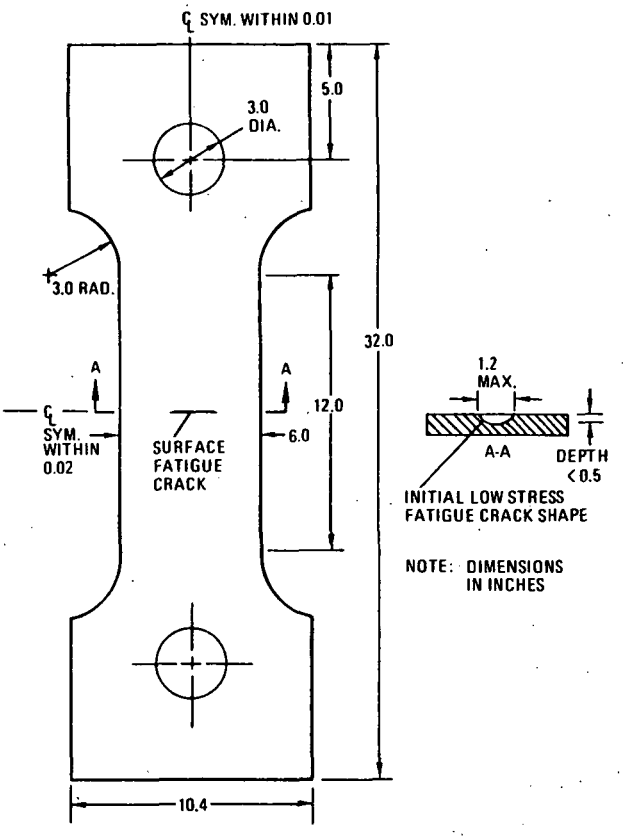

Figure 8. Specimen Configuration for Surface Crack Plane Strain Fracture Toughness and Cyclic Flaw Enlargement Tests

Specimen overall dimensions for both thicknesses were identical: 81.3 cm long by 26.4 cm wide (32 by 10.4 in.), with a 15.2 cm (6.0 in.) wide reduced test section. (See Figure 8.) However, the 0.318 cm (0.125 in.) thick specimens had a grip section 0.635 cm (0.25 in.) thick reduced to 0.318 cm (0.125 in.) in the test, while the 2.54 cm (1.0 in.) thick specimens were a constant thickness.

Surface cracks were made by machining a rectangular notch with a specially prepared electrode in an electrical discharge machine (EDM), followed by crack initiation in a semi-elliptical shape by fatigue cycling at 30 Hz. An attempt was made to obtain the following aspect ratios (a/2c) and flaw depth-to-thickness ratios (a/t) for various test conditions.

Techniques developed under a 1972 Independent Research and Development Study (IRAD) on nondestructive testing were used to control the size, shape, and depth of the surface flaws. Empirical data obtained in that study permitted the careful selection of electrode shapes during the EDM notching routine, as well as the machine notch depth. Placing constraints on both aspect ratio and depth of cracks with such a wide range was difficult, but the results obtained were reasonable. Control of the precrack was accomplished by a combination of axial and bending fatigue.

Specimen Thickness (cm)	(in.)	Orientation	Test	Temperature (°K)	(°F)	a/2c	a/t
2.54	1.0	L(1A)	Static	297	75	0.25	0.25
2.54	1.0	L(1A)		297	75	0.40	0.40
2.54	1.0	L(1A)		297	75	0.50	0.50
2.54	1.0	L(1A)		78	-320	0.25	0.25
2.54	1.0	L(1A)		78	-320	0.40	0.40
2.54	1.0	L(1A)		78	-320	0.50	0.50
2.54	1.0	LT(2B)		297	75	0.25	0.25
2.54	1.0	LT(2B)		297	75	0.40	0.40
2.54	1.0	LT(2B)		297	75	0.50	0.50
2.54	1.0	LT(2B)		78	-320	0.25	0.25
2.54	1.0	LT(2B)		78	-320	0.40	0.40
2.54	1.0	LT(2B)		78	-320	0.50	0.50
0.318	0.125	LT(2B)	Cyclic	297	75	0.10	0.10
0.318	0.125	LT(2B)		297	75	0.25	0.25
0.318	0.125	LT(2B)		297	75	0.40	0.40
0.318	0.125	LT(2B)		78	-320	0.10	0.10
0.318	0.125	LT(2B)		78	-320	0.25	0.25
0.318	0.125	LT(2B)		78	-320	0.40	0.40
2.54	1.0	LT(2B)		297	75	0.10	0.10
2.54	1.0	LT(2B)		297	75	0.25	0.25
2.54	1.0	LT(2B)		297	75	0.40	0.40
2.54	1.0	LT(2B)		78	-320	0.10	0.10
2.54	1.0	LT(2B)		78	-320	0.25	0.25
2.54	1.0	LT(2B)		78	-320	0.40	0.40

Static fracture tests were performed on twelve 2.54 cm (1.0 in.) thick specimens at room temperature and at 78°K (-320°F) in a 600,000-pound tensile test machine to obtain apparent plane-strain critical crack intensity factors. The tests at 78°K were accomplished by installing plastic bags around the specimens and directing liquid nitrogen into them.

Fracture surfaces were examined by light microscope to determine critical flaw shape and depth.

2.2.4 STIFFENED PANEL TESTS. To study the behavior of a crack emanating from a bolt hole, a total of 18 simulated stiffened panels were prepared (Figure 9) from the 8.26 cm (3.25 in.) plate of

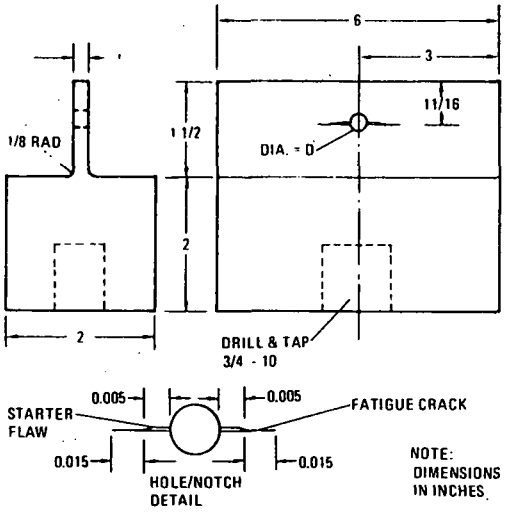

Figure 9. Stiffened Panels

2219-T87 aluminum. The conditions of testing (uncracked panels, cracked static panels, and fatigue cycled panels) are shown in Table 1. For the cracked specimens, a very small notch was induced on each side of the bolt hole with a manual grooving tool developed for this purpose. The specimens were oriented such that the expected path of the crack was in the same location as the longitudinal grain. The loading direction and the crack plane were selected to reproduce a crack growth similar to the fracture specimens designated ST(3A).

Table 1. Simulated Stiffened Panel Tests

Condition	Hole Diameter, D (cm)	(in.)	Thickness, t (cm)	(in.)	Replicates
			Static Tests		
Uncracked	0.635	0.250	0.318	0.125	1
Uncracked	0.635	0.250	1.270	0.500	1
Uncracked	1.270	0.500	1.270	0.500	1
Precracked	0.635	0.250	0.318	0.125	2
Precracked	0.635	0.250	1.270	0.500	2
Precracked	1.270	0.500	1.270	0.500	2
				Total	9
			Cyclic Tests		
Precracked	0.635	0.250	0.318	0.125	6
Precracked	0.635	0.250	1.270	0.500	6
Precracked	1.270	0.500	1.270	0.500	6
				Total	18

The uncracked panels were statically tested to failure first. The remainder of the panels was precracked at a load level of about 25 percent of the failure load of the uncracked panels.

Panels were designed with a rather large base to minimize localized bending of the outstanding leg. The base was drilled and tapped to accommodate a 3/4-10 pull rod that was easily adapted to either tensile or fatigue machines. The bolt hole was loaded by hardened steel pin attached to a double clevis (Figure 10). This arrangement was satisfactory for every case except the static tests of the 1.27 cm (0.5 in.) outstanding leg loaded by a 1/4 inch 0.635 cm (0.25 in.) diameter pin.

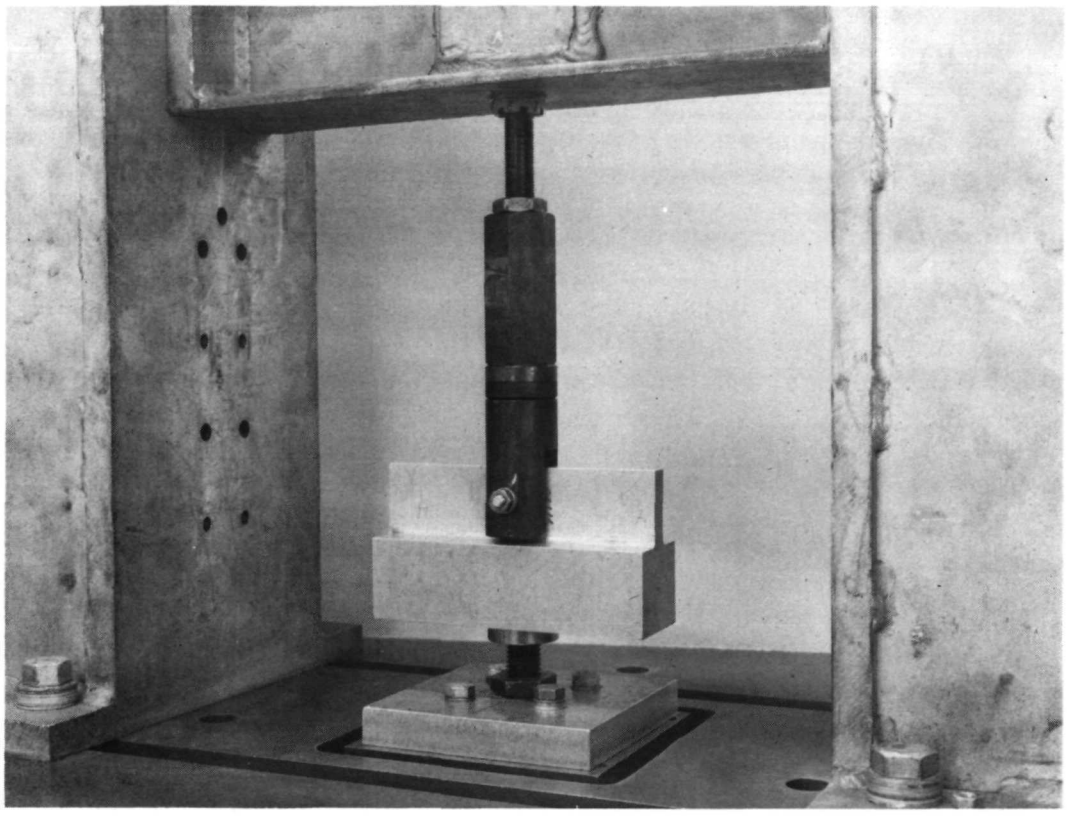

Figure 10. Simulated Test Panel

For static cracked tests, the critical crack size was determined by examining the specimen after fracture. For cyclic tests, all crack-measuring systems were unsatisfactory due to visual or noise interference from the loading pin or clevis. Cyclic tests were therefore interrupted periodically, the loading pin and clevis were removed, and the crack was measured visually in the unloaded condition. Cyclic tests were performed at about 40 and 70 percent of the precracked specimen static fracture load. All specimens were cycled a finite number of cycles and terminated.

2.2.5 CYCLIC TESTS. The cyclic tests specimens were subjected to a complex load spectrum (Figure 11) intended to provide more than one data point for each specimen. Precracking the machined notch was accomplished by using axial loads providing stress intensity ranges, ΔK, equal to 0.6 K_Q or 90 percent of the first scheduled cyclic growth ΔK, whichever was less. A frequency of 30 Hz and an R of +0.1 were used.

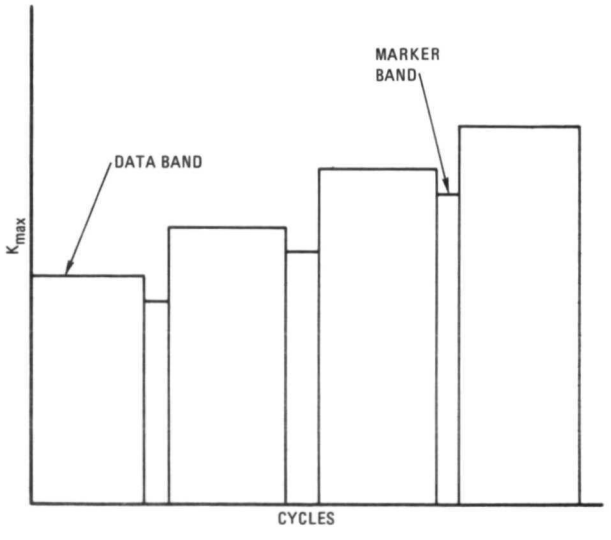

Figure 11. Graphical Representation of Cyclic Loading Sequence

Multiple values of cyclic stress crack growth were obtained by limiting crack growth at a specific value of ΔK ($\Delta K = K_{max} - K_{min}$) to about 0.0254 to 0.0127 cm (0.010 to 0.050 in.) at one of three frequencies and one load ratio, R (e.g., 1.0 Hz and R = +0.30). The cyclic growth obtained would then be marked by different axial cyclic loads and conditions (e.g., 0.9 ΔK, 5 Hz, and R = +0.10). Experience at Convair Aerospace has shown that this technique provides a fracture surface that can be readily measured to give accurate cyclic crack growth data and that eliminates the need for continued observation of the specimen surface to obtain growth measurements. Crack growth measurements have also been made by using plastic replicas of low-contrast fracture surfaces. Crack growth measurements made during testing by observing thick specimen surfaces are not accurate because of the curvature of the advancing crack front. In addition, crack growth in some instances (like sustained loading in an aggressive environment) will change from a slightly curved crack front to a tunneling mode. Tunneling cracks are not accountable in the presently available solutions for stress intensity and are, therefore, avoided by minimizing tunneling through limiting the increment of crack growth.

Experience with crackgrowth studies at Convair Aerospace has shown that one specimen can be used to obtain mulitple crack-growth data points. Crack growth tests were performed increasing values of ΔK (uphill ΔK), as shown in Figure 11. This approach eliminated any possibility of crack retardation caused by high values of ΔK followed by lower values of ΔK. However, crack growth occurring during the marker band portion of the test may be considered a qualitative test value of crack growth at the respective ΔK, R, and frequency used during cyclic marking. Any cyclic test specimen that survived the fourth data band was subsequently tested to failure statically to obtain K_Q.

Load-versus-deflection curves were obtained using the displacement gage shown in Figure 7 following the procedures given in ASTM E399 (Reference 10) to determine the pop-in or conditional load value, P_Q.

With some materials, the DCB specimen provides a sawtooth load-versus deflection curve, caused by pop-in critical crack growth, at K_Q and crack arrest, at K_{Ia} (References 3 and 4). Other materials exhibit crack growth by a slow tearing process and are recorded on the load-versus-deflection curve as a wavy line of small amplitude and as decreasing in load. To resharpen and reshape the crack front, the specimen were again cyclically loaded in the manner used for precracking.

The sustained stress crack growth tests were performed with precracked specimens. Precracking was performed in the manner described for the cyclic stress portion. Sustained stress was determined on the basis of initial stress intensity factor, K_{Ii}. Since each test specimen was used to obtain multiple data points, the loads were selected so as to obtain increasing values of K_{Ii}. A range of 0.025 to 0.125 cm (0.010 to 0.050 in.) was the goal for the sustained stress crack growth tests to avoid

tunneling of cracks. Studies in sustained load crack growth by Kropp (Reference 13) and others have shown that tunneling cracks can become large in short periods of time. However, additional axial cyclic loading will flatten the advancing crack front.

2.3 DATA REDUCTION

2.3.1 TENSILE TESTS. Data obtained in tensile testing was derived from stress/strain curves and physical measurements of the test specimens. Elongation (%) was obtained over a 5.1 cm (2.0 in.) gage length for longitudinal and long transverse specimens and over a 3.8 cm (1.5 in.) gage length for short transverse specimens. Tensile yield strength was obtained using the 0.2-percent offset method. Strength and modulus values were obtained by dividing the appropriate load by the pretest specimen dimensions.

2.3.2 FRACTURE TESTS. Calculations for fracture values were obtained using existing formulas with some slight modifications. Compliance gages were attached to the integral knife edges of the compact and DCB specimens. Plots of load variation with compliance gage output were recorded either on the drum of the tensile machine or by external X-Y recorders.

Crack growth of 0.318 cm (0.125 in.) thick specimens was measured visually with stainless steel scales and stereomicroscopes. Flaw growth on 2.54 cm (1.0 in.) thick specimens were determined after fracture with stereomicroscopes aided by polarized light in a manner described by ASTM Standard E399. Critical flaw size and shapes for part-through crack specimens were similarly measured after fracture.

2.3.2.1 Compact and Double Cantilever Beam Specimens

a. Compact Specimens. The solution for the opening mode stress intensity factor, K_I, is:

$$K_I = Y \frac{P\sqrt{a}}{BW}$$

For side-grooved specimens, the solution is:

$$K_I = Y \frac{P\sqrt{a}}{W\sqrt{B_N}}$$

where

Y = the dimensionless compliance parameter (References 11 and 12)

P = applied load (maximum value for K_X tests)

a = crack length measured from centerline of loading pin holes

W = specimen width measured from centerline of loading pin holes to back surface of specimen

B = specimen thickness

B_N = net or notch thickness equal to 0.9B

b. Double Cantilever Beam Tests. The 5-percent secant offset method (Reference 10) was used to obtain a conditional load value to calculate a conditional value (K_Q) of plane strain fracture toughness (K_{Ic}).

Values for all opening mode stress intensities (K_I) for DCB tests were determined by using the equation developed by Mostovoy et al. (Reference 4):

$$K_I^2 = \frac{4P^2}{b_N b h^3} \left[3 (a + a_o)^2 + h^2 \right]$$

where

P = applied load

b = width of specimen

b_N = 0.9b

h = half specimen height

a = crack length

a_o = an empirical rotation correction approximately equal to 0.6h for h values from 1.27 to 10.16 cm (0.5 to 4 in.) and values of a up to 25.4 cm ((10.0 in.).

2.3.2.2 Part-Through Crack Specimen. The maximum value of stress intensity factor (K_I) occurs at the end of the semiminor axis of the semielliptical flaw. Irwin's equation for K_I was used to calculate the conditional K_Q for all surface flaw specimens tested. The equation for K_I is given by:

$$K_I = \sigma_G M_{MSC} \sigma \sqrt{\pi} \sqrt{\frac{a}{Q}}$$

where

σ_G = gross area tension stress applied

a = precracked or initial depth of surface flaw

Q = surface flaw shape parameter obtainable from prepared curves or equations

M_{MSC} = NASA stress intensity magnification factor obtainable from published literature

Values of K_Q can be adjusted for the plastic zone (r_y) by using the following equations.

$$r_y = \frac{1}{4\sqrt{2\pi}} \left(\frac{K_Q}{\sigma_{ys}} \right)^2$$

and

$$a = a_o + r_y$$

where

r_y = plastic zone size

σ_y = yield strength at 0.2 percent offset at test temperature

a_i = measured crack depth

a = plastic zone adjusted crack length

SECTION 3

TEST RESULTS

3.1 MECHANICAL AND METALLOGRAPHIC TESTS

Results of tensile testing are shown in Table 2 for 297°K (75° F), 422°K (300° F0, 78°K (-320° F) and 20°K (-423° F). The location in the two plates (A or B) from which the tensile specimens were machined as shown, along with the location through the thickness. In all cases for a single location (for example, location A-14), the tensile specimens were excised from a single piece of material sawed from that location in that plate. In general, the tensile test specimen location was between two areas of fracture test specimen locations. Strength values of the material at room temperature 214°K (75° F) exceed minimum specification for 2219-T87 aluminum in the 8.26 cm (3.25 in.) thickness.

There is very little difference between grain orientations as far as ultimate tensile strength is concerned. In fact, the only significant difference in the material at room temperature occurs in elongation and reduction in area, where the short transverse grain direction shows considerably lower reduction in area and somewhat lower elongation. Although some of the lower elongation may be attributed to a smaller gage length, these low values hint at the possibility of embrittlement in that grain direction.

As expected, the strength of the alloy at 422°K (300° F) was lower than at room temperature, but at lower temperatures the tensile strengths showed a significant increase. In general, elongation did not show a decrease with a decrease in temperature, indicating that this alloy may be tough at those temperatures. On the other hand, the short transverse specimens had a tendency to fail in the threaded grip sections, suggesting notch sensitivity or embrittlement at 78°K (-320° F) and 20°K (-423° F).

Except at room temperature, the modulus of elasticity values were quite erratic. In some cases, stress/strain curves were so inconsistent that it was impossible to obtain modulus values using normal graphic techniques.

Metallographic samples were taken from each plate and examined. The structure is shown in Figure 12, which indicates that the plate grains are equiaxed on the surface but shortened in the thickness direction. The structure resembles a forging where the effect of the working is to decrease the thickness with no strong planer directionality.

Knoop hardness tests were run on specimens from each of the faces. The equivalent Rockwell B hardness values averaged 74.5 to 76.5, with the top surface exibiting the lowest hardness.

Table 2. Strength of 2219-T87 Aluminum Alloy at Various Temperatures

I.D.	Location Length	Location Thickness	F_{tu} (MN/m^2)	F_{tu} (ksi)	F_{ty} (0.2) (MN/m^2)	F_{ty} (0.2) (ksi)	e 5.08 cm, 2.0 in. (%)	R.A. (%)	E (GN/m^2)	E ($psi \times 10^6$)
297° K (75° F)										
A14 L-T	A14	Top	487	70.6	382	55.4	11.0	15.1	73.8	10.7
A14 L-M	A14	Middle	473	68.6	372	53.9	11.5	19.3	76.5	11.1
A14 ST1	A14	-	478	69.3	376	54.5	8.0*	7.6	71.7	10.4
A14 ST2	A14	-	478	69.3	376	54.5	8.0*	7.6	71.7	10.4
A22 L-M	A22	Middle	467	67.7	368	53.4	11.5	15.1	75.2	10.9
A22 ST2	A22	-	478	69.3	376	54.5	8.0*	6.7	75.2	10.9
B10 LT-T	B10	Top	476	69.1	381	55.2	11.0	15.5	73.8	10.7
B10 ST-2	B10	-	474	68.8	376	54.5	7.0*	7.6	70.3	10.2
B18 L-B	B18	Bottom	476	69.0	376	54.6	12.0	18.4	70.3	10.2
B18 LT-M	B18	Middle	481	69.8	378	54.8	11.0	9.7	79.3	11.5
B10 LT-M	B10	Middle	478	69.3	377	54.7	11.5	9.6	75.2	10.9
422° K (300° F)										
A14 LB	B14	Bottom	379	55.04	324	46.93	10.0	30.6	91.0	13.2
A14 LTM	A14	Middle	378	54.80	312	45.21	8.0	22.6	90.3	13.1
A14 ST2	A14	-	398	57.79	344	49.85	11.0*	10.9	-	-
A22 L-B**	A22	Bottom	-	-	228	33.05	-	57.2	91.0	13.2
A22 LT T	A22	Top	399	57.83	284	51.20	10.0	24.0	95.8	13.9
A22 ST1**	A22	-	308	44.66	284	51.16	5.0*	28.4	-	-
B10 ST1	B10	-	389	56.44	320	46.45	10.0*	14.6	-	-
B18 LT-B	B18	Bottom	348	50.42	312	45.31	11.0	34.2	104.1	15.1
78° K (-320° F)										
A14 LT-T	A14	Top	581	84.3	453	65.7	12.0	15.1	84.8	12.3
A14 LT-B	A14	Bottom	592	85.8	439	63.7	11.0	12.9	67.6	9.8
A22 LT-M	A22	Middle	592	85.8	439	63.7	10.0	16.5	90.3	13.1
A22 ST-3	A22	-	574	83.2	413	59.9	8.0*	5.5	55.2	8.0
B10 L-T	B10	Top	560	81.2	430	62.4	15.0	29.4	88.9	12.9
B10 L-B	B10	Bottom	587	85.1	444	64.4	14.0	19.1	114	16.5
B10 LT-B	B10	Bottom	463	81.7	434	62.9	14.5	25.1	91.0	13.2
B10 ST-3†	B10	-	567	82.2	425	61.6	-	-	72.4	10.5
B10 L-M	B10	Middle	463	81.7	432	62.6	16.0	28.8	73.8	10.7
20° K (-423° F)										
A22 L-T	A22	Top	659	95.6	566	82.1	12.5	16.9	-	-
A22 LT-B	A22	Bottom	595	86.3	465	67.4	11.0	11.1	71.7	10.4
B18 L-T	B18	Top	647	93.8	490	71.0	15.5	13.4	86.2	12.5
B18 L-M	B18	Middle	576	83.6	456	66.2	15.5	17.4	73.1	10.6
B18 LT-T	B18	Top	717	104.0	526	76.3	15.0	13.4	73.8	10.7
B18 LT-1	B18	-	633	91.8	461	66.8	6.7*	13.0	64.8	9.4
B18 ST-2†	B18	-	607	88.0	480	69.6	-	-	-	-
B18 ST-3†	B18	-	581	84.3	485	70.4	-	-	-	-

* In 3.81 cm (1.5 in.) gage length

** Failed outside gage mark.

† Failed in threads.

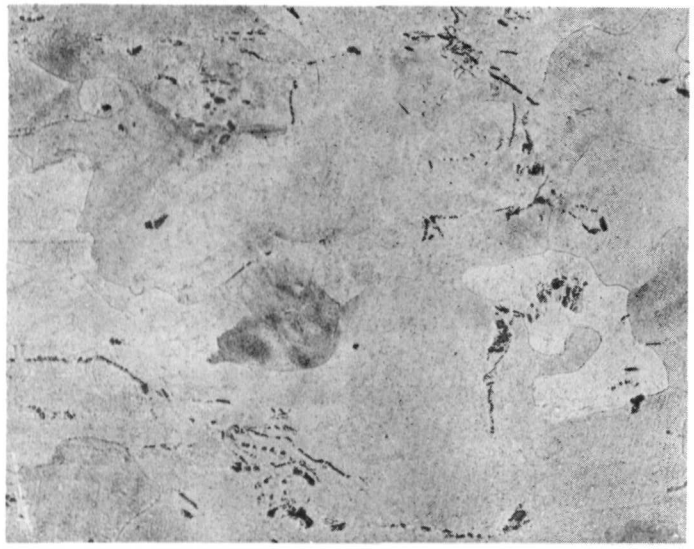

a. TOP

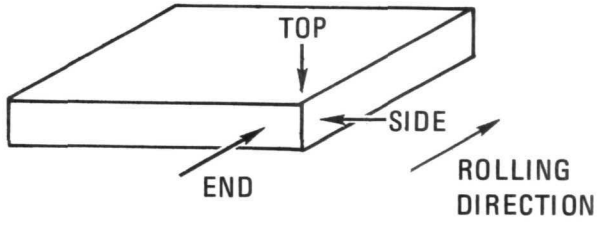

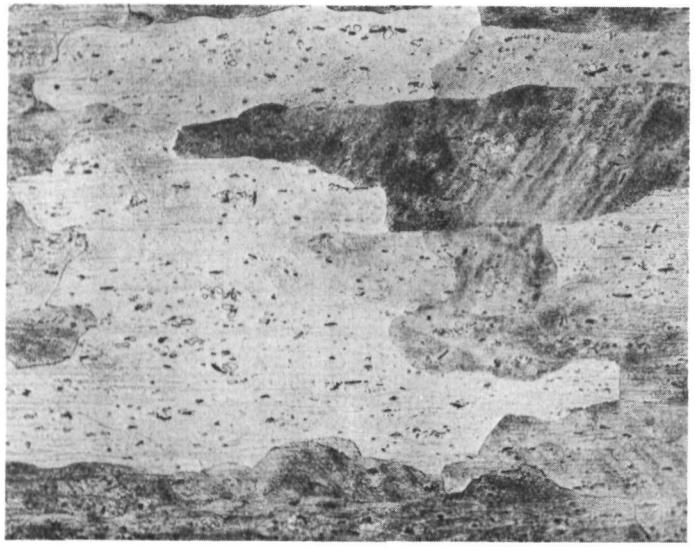

b. END

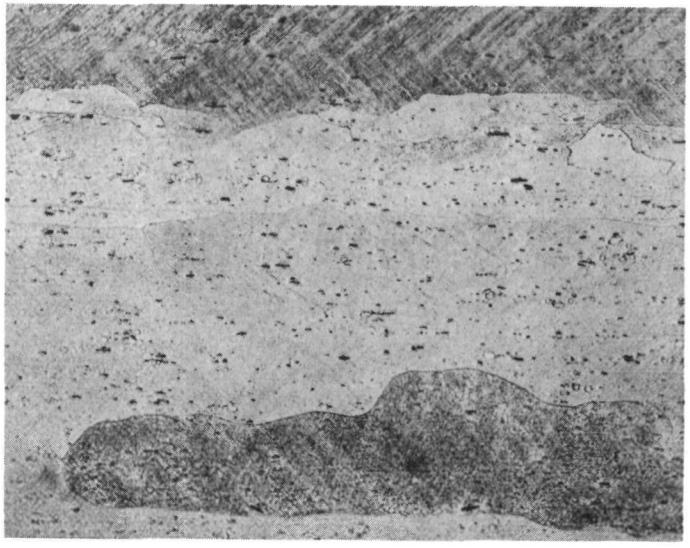

c. SIDE

Figure 12. Microstructure of 2219-T87 Plate

Crack growth in several longitudinal and long transverse specimens changed direction during the test. The metallographic structure suggests that this could be associated with grain boundaries, but it could be due to a texture developed during working.

3.2 FRACTURE TESTS

3.2.1 CYCLIC FLAW GROWTH. Cyclic flaw growth variation with ΔK was determined for the six grain/crack plane combinations in air at 50 percent relative humidity (Figure 13). The bulk of the data was obtained at a constant cyclic frequency of 1.0 Hz, but some additional information was obtained at 0.1 and 10.0 Hz for 2219-T87 aluminum alloy loaded in the short transverse direction (designated as ST(3A) in Figure 1).

The test sequence was similar for each specimen, although ΔK values had a large range for the stronger orientations such as the longitudinal L(1A) specimens. In general, each specimen was subjected to four loading steps, called data bands, separated by three loading steps, known as marker bands. The marker bands were designed to provide distinct boundaries for each data band when growth measurements were made after fracture. Crack growth was usually readily observed on the surface of the 0.318 cm (0.125 in.) specimens, and the marker bands became academic.

To eliminate the potential variable of retardation, the sequence of loading required that no data band load be less than the preceding load. The marker band varied from the data band in that 1) ΔK was lower, 2) stress ratio, R, was lower, 3) cyclic frequency was higher, and 4) fewer cycles were applied. For example, the following loading step was typical for tests at 1.0 Hz.

	Load (lb)	Stress Ratio	Frequency (Hz)	No. of Cycles
Data Band	1000	R = 0.3	1.0	7600
Marker Band	900	R = 0.1	5.0	1000

The exact ΔK was initially called out in advance for each band, but because of the difficulty of predicting the exact crack growth in a given number of cycles, it was impossible to determine the exact applied ΔK for the second and subsequent steps. Consequently, the sequence was prepared based on progressively larger loads, which provided larger ΔK whether or not crack growth was significant. When specimens survived all cyclic load steps, they were statically loaded to failure to obtain critical stress intensity factors.

For plotting purposes, initial and final ΔK values were calculated for each data band (using initial and final crack size), and the average value was determined. To obtain average crack growth, da/dN, total growth for each data band was divided by the number of cycles to produce that growth. Average ΔK was then plotted against average da/dN on a log/log scale as shown in Figure 13a. Although crack sizes varied between

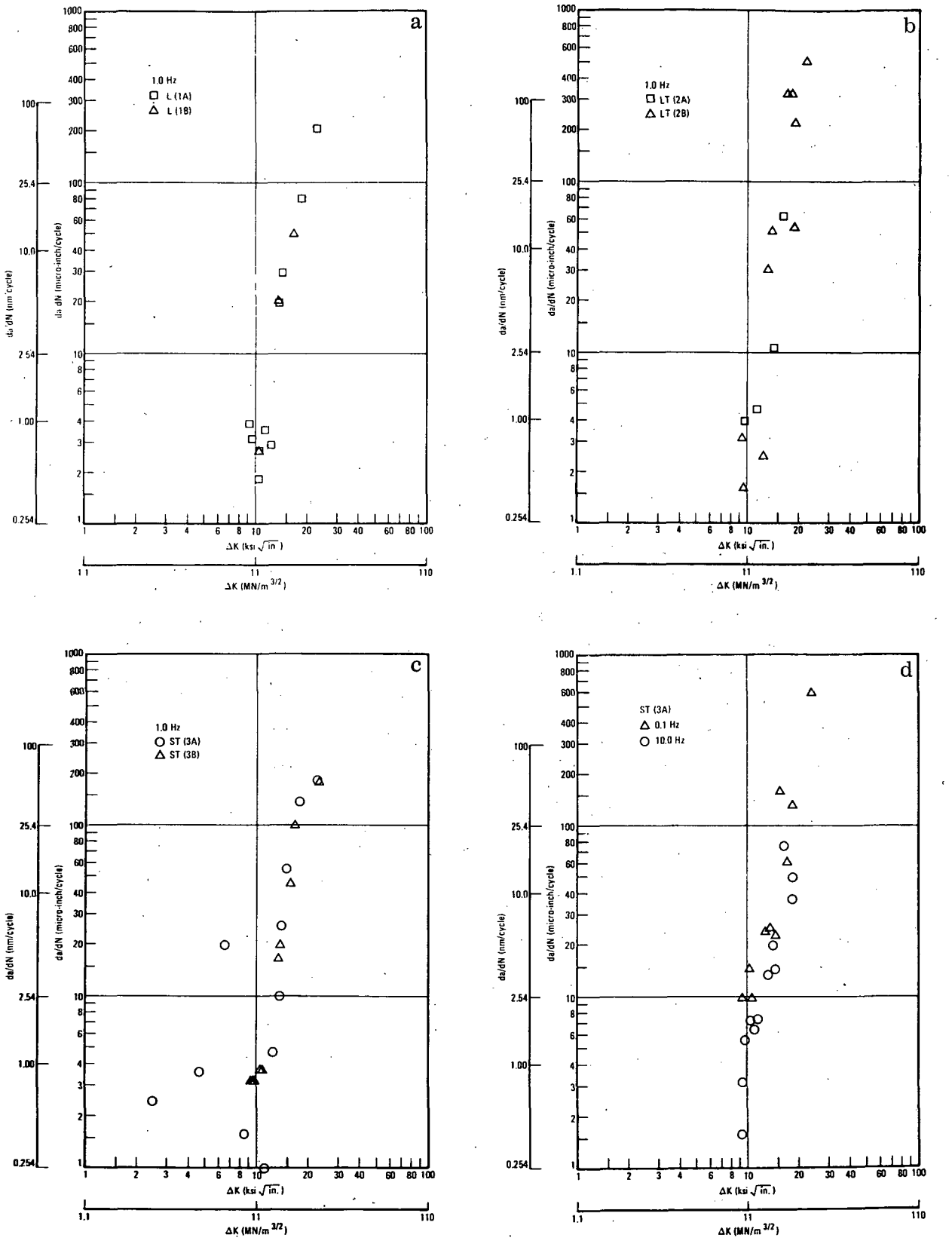

Figure 13. Crack Growth Variation with ΔK for 2219-T87 Aluminum in Air at 50 Percent Relative Humidity, 0.318 cm (0.125 in.)

specimens, it appeared that the ratio of the log of ΔK to the log of a da/dN was constant for a given direction of loading. In Figure 13a, for example, a single straight line describes the curves for L(1A) and L(1B). The LT(2A) and LT(2B) specimens provide similar results, as do ST(3A) and ST(3B).

Earlier testing suggested that Specimen ST(3A) would be the orientation with the minimum toughness or resistance to crack growth. Consequently, this specimen orientation was used to obtain more detailed data. In this portion of the study, the ST(3A) specimen was used to study the effect of cyclic frequency on the cyclic crack growth rate (da/dN). The two frequencies selected were 0.1 and 10 Hz. While the difference is small (Figure 13d), it appears that crack growth per cycle is larger at 0.1 than at 10.0 Hz for a given ΔK. This result is expected in an environment that is aggressive to the test alloy. That is, at a very slow cyclic rate, the environment has a sufficient time to cause crack growth at load, as in a sustained load test. Assuming that the result is not an anomaly or statistical inaccuracy, it is assumed that the 2219-T87 aluminum alloy is vulnerable to increased crack growth in air at 50 percent relative humidity.

3.2.2 PLANE STRESS CRITICAL CRACK INTENSITY FACTOR. Static fracture toughness values obtained from 0.318 cm (0.125 in.) fracture specimens are shown in Table 3 for tests in liquid nitrogen and in Table 4 for room temperature air after prior exposure. As exhibited in other tests, toughness of the longitudinal and long transverse specimens is significantly greater than for short transverse specimens. At liquid nitrogen temperature, the longitudinal L(1A) specimens and the LT(2B) specimens seem to provide the highest toughness. In the short transverse specimens, the difference is small as far as the propagating crack direction is concerned.

As mentioned, those specimens that survived cyclic or sustained load exposures were subsequently statically loaded to failure. Results of these tests are shown in Table 4. It appears that in virtually all cases, specimens cycled in air tended to exhibit lower "residual" fracture toughness than corresponding specimens loaded in a 3.5-percent NaCl solution. It can be argued that the cyclic specimens were subjected to greater crack growths than were the sustained load specimens.

Sustained load specimens, however, were subjected to low stress high frequency fatigue loading between load steps to minimize crack blunting. In these cases, cyclic flaw growth was minimal.

Again, conditional loads (P_Q) and maximum loads (P_{max}) were higher for the sustained load test specimens than for the corresponding cyclic loaded specimens. The data strongly suggests that the exposure in salt water under sustained load has a blunting effect that retards crack growth and inhibits susceptibility to the brittle fracture phenomenon.

Table 3. Plane Stress Critical Crack Intensity Factor for 2219-T87 in Liquid Nitrogen, 0.318 cm (0.125 in.) Fracture Specimens

Specimen Identification	Critical Crack Length, a (cm)	(in.)	Conditional Crack Intensity Factor, K_x ($MN/m^{3/2}$)	(ksi$\sqrt{in.}$)	Load at 5% Secant, P_Q (MN)	(lb)	Maximum Load, P_{max} (MN)	(lb)
A29 L(1A)1	2.3	0.91	62.2	56.6	0.00721	1620	0.01112	2500
A29 L(1A)4	2.4	0.94	71.4	65.0	0.00805	1810	0.01019	2290
A29 L(1B)1	2.5	0.98	44.8	40.8	0.00487	1095	0.00698	1570
A29 LT(2A)1	2.5	0.97	53.6	48.8	0.00587	1320	0.00721	1620
A27 LT(2B)1	2.3	0.91	51.1	46.5	0.00592	1330	0.00761	1710
A27 LT(2B)4	2.3	0.91	65.7	59.8	0.00770	1730	0.00814	1830
A29 ST(3A)1	2.3	0.90	36.5	33.2	0.00427	960	0.00434	975
A29 ST(3A)4	2.3	0.92	35.9	32.7	0.00414	930	0.00449	1010
A29 ST(3A)7	2.3	0.91	32.5	29.6	0.00376	846	0.00405	910
A27 ST(3B)1	3.2	1.25	35.3	32.1	0.00289	650	0.00309	695
A27 ST(3B)4	2.3	0.90	37.2	33.9	0.00436	980	0.00485	1090
A27 ST(3B)7	2.4	0.95	36.0	32.8	0.00403	907	0.00500	1125

Table 4. Static K_x Values After Cyclic or Sustained Load Exposure, 0.318 cm (0.125 in.) Fracture Specimens

Specimen Identification	Cyclic (Hz)	Sustained	Environment	K_x ($MN/m^{3/2}$)	(ksi $\sqrt{in.}$)	P_Q (MN)	(K)	P_{max} (MN)	(K)
A29 L(1A)5	1		Air, 50% RH	63.1	57.4	0.00627	1.41	0.00841	1.89
A29 L(1A)2	1		Air, 50% RH	55.3	50.3	0.00556	1.25	0.00854	1.92
A29 L(1A)3		X	3.5% NaCl	66.4	60.4	0.00654	1.47	0.00947	2.13
A29 L(1A)6		X	3.5% NaCl	71.0	64.6	0.00685	1.54	0.00863	1.94
A29 L(1B)2	1		Air	48.8	44.4	0.00405	0.91	0.00538	1.21
A29 L(1B)3		X	3.5% NaCl	74.8	68.1	0.00578	1.30	0.00645	1.45
A2 LT(2B)5	1		Air	67.8	61.7	0.00667	1.50	0.00814	1.83
A27 LT(2B)2	1		Air	56.5	51.4	0.00556	1.25	0.00778	1.75
A27 LT(2B)3		X	3.5% NaCl	70.4	64.1	0.00694	1.56	0.00814	1.83
A27 LT(2B)6		X	3.5% NaCl	70.4	64.1	0.00730	1.64	0.00912	2.05
A29 LT(2A)2	1		Air	44.6	40.6	0.00378	0.85	0.00480	1.08
A29 LT(2A)3		X	3.5% NaCl	53.4	48.6	0.00547	1.23	0.00605	1.36
A27 ST(3B)2				45.1	41.0	0.00311	0.70	0.00316	0.71
A27 ST(3B)5	1		Air	31.8	28.9	0.00222	0.50	0.00289	0.65
A27 ST(3B)8	1		Air	35.6	32.4	0.00302	0.68	0.00369	0.83
A27 ST(3B)6		X	3.5% NaCl	47.7	43.4*	-	-	0.00400	0.90
A27 ST(3B)9		X	3.5% NaCl	48.8	44.4			0.00400	0.90
A27 ST(3B)3		X	3.5% NaCl	43.0	39.1	0.00391	0.88	0.00449	1.01
A29 ST(3A)8	1		Air	34.4	31.3	0.00294	0.66	0.00347	0.78
A29 ST(3A)2	1		Air	34.8	31.7	0.00271	0.61	0.00316	0.71
A29 ST(3A)5	1		Air	36.6	33.3	0.00271	0.61	0.00285	0.64
A29 ST(3A)3		X	3.5% NaCl	47.1	42.9	0.00423	0.95	0.00463	1.04
A29 ST(3A)6		X	3.5% NaCl	42.6	38.8*	-	-	0.00378	0.85
A29 ST(3A)9		X	3.5% NaCl	54.1	49.2*	-	-	0.00378	0.85
A11 ST(3A)6	1		Air	38.7	35.2	0.00285	0.64	0.00307	0.69
A11 ST(3A)5	1		Air	34.6	31.5	0.00294	0.66	0.00374	0.84
A11 ST(3A)4	1		Air	38.5	35.0	0.00276	0.62	0.00302	0.68
A11 ST(3A)3	1		Air	34.4	31.3	0.00311	0.70	0.00383	0.86
A11 ST(3A)2	1		Air	43.7	39.8	0.00231	0.52	0.00245	0.55
A11 ST(3A)1	1		Air	36.7	33.4	0.00214	0.48	0.00240	0.54

* Failed under sustained load. K_x calculated using maximum load and corresponding crack size.

3.2.3 DOUBLE CANTILEVER BEAM (DCB) CYCLIC TESTS. Initial constraints of this program included plate thickness, 8.26 cm (3.25 in.), and the thickness requirement, 2.54 cm (1.0 in.) for comparative plane strain data. Unfortunately, these requirements worked against the program in various grain orientations. Where the crack was required to traverse the longitudinal grain, fractures were unpredictable and usually in a plane parallel to the direction of loading. The most critical of these orientations was L(1A), where the load was applied in the direction of the longitudinal grain in the plate. During initial tests of L(1A) specimens, pre-cracking proceeded normally and crack growth was observed during cycling at 1 Hz, although da/dN values were well below that expected. After four ΔK steps were applied at room temperature (50-percent relative humidity), the specimen was statically tested to failure. The fracture occurred parallel to the direction of loading (referred to as vertical cracking as opposed to the expected horizontal crack growth in a test machine). Observation of the fractured surface with a light microscope revealed that although the crack had propagated on the surface in the vicinity of the face groove, it had changed directions in the center of the specimen and failed in a plane parallel to load application.

Several attempts were made to use the L(1A) specimens by modifying the geometry (such as deepening the surface groove or making chevron cuts at the leading edge of the crack), but none provided sufficient crack growth in the right plane for useful data.

In general, crack growth was most satisfactory in the short transverse ST(3A), ST(3B) specimens, where it was in the plane of longitudinal rolling direction and the long transverse direction (Tables 5 through 7).

Cyclic tests were performed at room temperature (50-percent relative humidity), 78° K (-320° F), and 422° K (300° F) at 1.0 Hz for all specimen orientations. In addition, ST(3A) specimens were tested at the three temperatures at 0.1 and 10 Hz.

Most cyclic tests were discontinued after three ΔK steps to obtain static fracture toughness values. Some tests failed at lower loads, while others were continued into the fourth step if it was considered likely that the specimen would survive. All cylic data for the DCB is shown in Tables 5 through 7, with significant data plotted in Figures 14 and 15. Crack growth was much harder to read for these specimens than for the 0.318 cm (0.125 in.) specimens.

The first crack length value listed in the tables (a_o) is that after pre-cracking. The ΔK values are averages obtained from adding the ΔK at the beginning of a load step to the ΔK at the end of that load step and dividing by two. Crack growth rates were obtained by dividing the crack growth for a given load step by the number of cycles required to drive the crack that distance.

Generally, the number of cycles per load step decreased as a specimen test progressed so that crack growth would be similar for each ΔK. In some cases, it was impossible

Table 5. Cyclic Crack Growth for 2219 Aluminum at 297°K (Room Temperature), 2.54 cm (1.0 in.) DCB

Specimen ID	Frequency (CPS)	a_o (in)	a_o (cm)	ΔK_1 ksi $\sqrt{in}$	ΔK_1 $MN/m^{3/2}$	a_1 (in)	a_1 (cm)	da/dN in/cy	da/dN nm/c	N (Cycles)	ΔK_2 ksi $\sqrt{in}$	ΔK_2 $MN/m^{3/2}$	a_2 (in)	a_2 (cm)	da/dN in/c	da/dN nm/c	N (Cycles)	ΔK_3 ksi $\sqrt{in}$	ΔK_3 $MN/m^{3/2}$	a_3 (in)	a_3 (cm)	da/dN in/c	da/dN nm/c	N (Cycles)	ΔK_4 ksi $\sqrt{in}$	ΔK_4 $MN/m^{3/2}$	a_4 (in)	a_4 (cm)	da/dN in/c	da/dN mn/c	N (Cycles)
A3 L(1B)2	1.0	1.17	2.97	10.2	11.2	1.26	3.20	12.5	318	7200							5400	18.3	20.1	1.39				800	20.9	23.0	1.40	3.56	167	4240	60
A7 LT(2A)1	1.0	1.09	2.77							7200	9.30	10.2	1.13	2.87			5400	12.9	14.2	1.14	2.90	1.25		800	15.7	17.3	1.17	2.97	500	12700	60
A11 ST(3A)1	1.0	1.22	3.10	12.1	13.3	1.90	4.83	16.3	414	41800																					
2	1.0	1.19	3.02	5.44	5.98	1.30	3.30	8.80	223	12500	10.4	11.4	1.35	3.43	10.4	264	8300	14.6	16.0	1.37	3.48	20.0		1000							
3	1.0	1.16	2.95	5.27	5.79	1.22	3.10	4.80	122	12500	10.0	11.0	1.28	3.25	7.23	184	8300	14.2	15.6	1.32	3.35	40.0		1000							
A9 ST(3B)1	1.0	1.13	2.87	11.2	12.3	1.59	4.04	12.5	318	38000	13.9	15.3	1.79	4.55	1.05	2670	1900														
2	1.0	1.11	2.82	5.15	5.66	1.19	3.02	6.40	163	12500	9.84	10.8	1.25	3.18	7.23	184	8300	13.7	15.1	1.28	3.25	30.0		1000	19.2	21.1	1.31	3.33	240	6100	125
3	1.0	1.10	2.79	5.03	5.53	1.12	2.84	1.60	40.6	12500	9.51	10.4	1.20	2.59	9.64	245	8300	13.5	14.8	1.23	3.12	30.0		1000	19.1	21.0	1.34	3.40	880	22400	125
A11 ST(3A)7	0.1	1.12	2.84	8.20	9.01	1.17	2.97	27.8	706	1800	12.4	13.6	1.20	2.59	16.7	424	1800	16.5	18.1	1.29	3.28	90.0		1000							
9	0.1	1.15	2.92	8.32	9.14	1.19	3.02	22.2	564	1800	12.6	13.8	1.23	3.12	22.2	564	1800	17.3	19.0	1.44	3.66	210		1000							
12	0.1	1.09	2.77	8.05	8.85	1.14	2.90	27.8	706	1800	12.3	13.5	1.20	2.59	33.3	846	1800	16.4	18.2	1.26	3.20	60.0		1000							
A11 ST(3A)13	10.0	1.15	2.92	5.17	5.68	1.16	2.95	.80	20.3	12500	9.73	10.7	1.24	3.15	9.52	242	8400	13.9	15.3	1.28	3.25	40.0		1000							
15	10.0	1.15	2.92	5.18	5.69	1.17	2.97	1.60	40.6	12500	9.73	10.7	1.23	3.12	7.14	181	8400	13.8	15.2	1.28	3.25	50.0		1000							
16	10.0	1.14	2.90	5.17	5.68	1.17	2.97	2.40	61.0	12500	9.79	10.8	1.25	3.18	9.52	242	8400	14.0	15.4	1.31	3.33	60.0		1000							

Table 6. Cyclic Crack Growth for 2219 Aluminum at 78°K (-320°F), 2.54 cm (1.0 in.) DCB

Specimen ID	Frequency (CPS)	a_o (in)	a_o (cm)	ΔK_1 ksi$\sqrt{in}$	ΔK_1 MN/m$^{3/2}$	a_1 (in)	a_1 (cm)	da/dN μin/cy	da/dN nm/c	N (Cycles)	ΔK_2 ksi$\sqrt{in}$	ΔK_2 MN/m$^{3/2}$	a_2 (in)	a_2 (cm)	dA/dN μin/cy	dA/dN nm/c	N (Cycles)	ΔK_3 (ksi$\sqrt{in}$)	ΔK_3 MN/m$^{3/2}$	a_3 (in)	a_3 (cm)	da/dN μin/c	da/dN nm/c	N (Cycles)	ΔK_4 (ksi$\sqrt{in}$)	ΔK_4 (MN/m$^{3/2}$	a_4 (in)	a_4 (cm)	da/dN μin/c	da/dN nm/c	N (Cycles)
A3 L(1B)8	1.0	1.08	2.74	4.97	5.46	1.10	2.79	1.39	35.3	14400	9.82	10.8	1.10	2.79			10000	13.0	14.3	1.17	2.97	5.56	141	12600							
A7LT(2A)7	1.0	1.08	2.74	4.94	5.43	1.08	2.74			14400	9.76	10.7			2.00	50.8	10000	13.0	14.3	1.18	3.00	6.35	161	12600	20.4	22.4	1.41	3.58	21.8	554	10564
A11 ST(3A)22	1.0	1.12	2.84	5.06	5.56	1.12	2.84			14400	10.0	11.0	1.15	2.92	3.00	76.2	10000	13.5	14.8	1.28	3.25	10.3	262	12600							
23	1.0	1.13	2.87	5.15	5.66	1.17	2.97	2.78	70.6	14400	10.6	11.6	1.29	3.28	12.0	305	10000	14.6	16.0	1.41	3.58	9.5	241	12600							
24	1.0	1.10	2.79	5.05	5.55	1.13	2.87	2.08	52.8	14400	10.1	11.1	1.15	2.92	2.00	50.8	10000	13.5	14.8	1.28	3.25	10.3	262	12600							
A9 ST(3B)22	1.0	1.09	2.77	4.97	5.46	1.09	2.77			14400	9.84	1.12	1.12	2.84	3.00	76.2	10000	13.4	14.7	1.27	3.22	11.9	302	12600							
23	1.0	1.09	2.77	4.97	5.46	1.09	2.77			14400	9.84	10.8	1.12	2.84	3.00	76.2	10000	13.2	14.5	1.21	3.07	7.14	181	12600							
24	1.0	1.09	2.77	4.97	5.46	1.09	2.77			14400	9.84	10.8	1.12	2.84	3.00	76.2	10000	13.2	14.5	1.22	3.10	7.94	262	12600							
A11 ST(3A)17	0.1	1.10	2.79	5.06	5.56	1.14	2.90	2.78	70.6	14400	10.1	11.1	1.17	2.92	3.00	76.2	10000	13.4	14.7	1.21	3.07	6.67	169	6000							
18	0.1	1.09	2.77	5.03	5.53	1.13	2.87	2.78	70.6	14400	10.2	1.20	1.20	3.05	7.00	178	10000	13.6	14.9	1.24	3.15	6.67	169	6000							
14	0.1	1.11	2.82	5.12	5.63	1.17	2.97	4.17	106	14400																					
A11 ST(3A)6	10.0	1.08	2.74	4.94	5.43	1.08	2.74			18440	9.82	10.8	1.11	2.82	3.00	76.2	10000	13.2	14.5	1.23	3.12	9.52	242	12600							
8	10.0	1.08	2.74	4.94	5.43	1.08	2.74			14400	9.88	10.9	1.13	2.87	5.00	123	10000	13.2	14.5	1.20	3.05	11.7	297	6000							
11	10.0	1.09	2.77	4.97	5.46	1.09	2.77			14400	9.94	10.9	1.15	2.92	6.00	152	10000	13.3	14.6	1.22	3.10	11.7	297	6000							

Table 7. Cyclic Crack Growth for 2219 Aluminum at 422°K (300°F), 2.54 cm (1.0 in.) DCB

Specimen ID	Frequency (CPS)	a_o (in)	a_o (cm)	K_1 ksi$\sqrt{in}$	K_1 MN/m$^{3/2}$	a_1 (in)	a_1 (cm)	da/dN μin/cy	da/dN nm/c	N (Cycles)	K_2 ksi$\sqrt{in}$	K_2 NM/m$^{3/2}$	a_2 (in)	a_2 (cm)	da/dN μin/c	da/dN mn/c	N (Cycles)	K_3 ksi$\sqrt{in}$	K_3 NM/m$^{3/2}$	a_3 (in)	a_3 (cm)	da/dN μin/c	da/dN nm/c	N (Cycles)	K_4 ksi$\sqrt{in}$	K_4 NM/m$^{3/2}$	a_4 (in)	a_4 (cm)	da/dN μin/c	da/dN nm/c	N (Cycles)
A3 L(1B)5	1.0	1.18	3.00	10.2	11.3	1.31	3.33	18.1	460	7200																					
A7 LT(2A)11	1.0	1.11	2.82	5.08	5.58	1.14	2.90	4.17	106	7200	9.50	10.4	1.17	2.47	5.56	141	5400	13.2	14.5	1.18	3.00	12.5	318	800	16.2	17.8	1.23	3.12	833	21 200	60
A11 ST(3A)13	1.0	1.16	2.95	5.36	5.88	1.28	3.25	16.7	424	7200	10.2	11.2	1.30	3.30	3.70	94.0	5400	14.5	15.9	1.38	3.51	100	2540	800							
14	1.0	1.12	2.84	5.15	5.65	1.18	3.00	8.33	212	7200	9.76	10.7	1.23	3.12	9.26	235	5400	14.0	15.4	1.33	3.38	125	3175	800							
15	1.0	1.12	2.84	5.15	5.65	1.18	3.00	8.33	212	7200	9.79	10.7	1.24	3.15	11.1	282	5400	14.1	15.5	1.34	3.40	125	3175	800							
A9 ST(3B)13	1.0	1.11	2.82	5.06	5.56	1.13	2.87	2.78	70.6	7200	9.41	10.3	1.17	2.97	7.41	188	5400	13.4	14.7	1.21	3.07	50.0	1270	800	16.3	17.9	1.24	3.15	500	12700	60
14	1.0	1.10	2.79	5.05	5.54	1.13	2.87	4.17	106	7200	9.44	10.4	1.16	2.95	5.56	141	5400	13.2	14.5	1.19	3.02	37.5	953	800	16.2	17.8	1.23	3.12	667	16900	60
15	1.0	1.11	2.82	5.09	5.59	1.15	2.92	5.56	141	7200	9.60	10.5	1.20	3.05	9.26	235	5400	13.7	15.0	1.28	3.25	100	2540	800							
A11 ST(3A) 1	0.1	1.12	2.84	8.27	9.08	1.20	3.05	4.44	1130	1800	12.7	13.9	1.25	3.18	27.8	706	1800	16.9	18.6	1.32	3.35	70.0	1778	1000							
2	0.1	1.08	2.74	8.00	8.78	1.13	2.87	27.8	706	1800	12.2	13.4	1.17	2.97	22.2	564	1800														
10	0.1	1.07	2.72	7.96	8.74	1.12	2.84	27.8	706	1800	12.2	13.4	1.19	3.02	38.9	988	1800	16.5	18.1	1.29	3.28	100	2540	1000							
A11 ST(3A)3	10.0	1.10	2.79	5.11	5.61	1.17	2.97	5.60	142	12500	9.65	10.6	1.20	3.05	3.57	90.7	8400	13.5	14.8	1.23	3.12	30.0	762	1000							
5	10.0	1.13	2.87	5.18	5.69	1.19	3.02	4.80	122	12500	9.87	10.8	1.26	3.20	8.33	212	8400	14.2	15.6	1.35	3.43	90.0	2286	1000							
4	10.0	1.12	2.84	5.17	5.68	1.19	3.02	5.60	142	12500	9.73	10.7	1.21	3.07	2.38	60.5	8400	13.7	15.0	1.26	3.20	50.0	1270	1000							

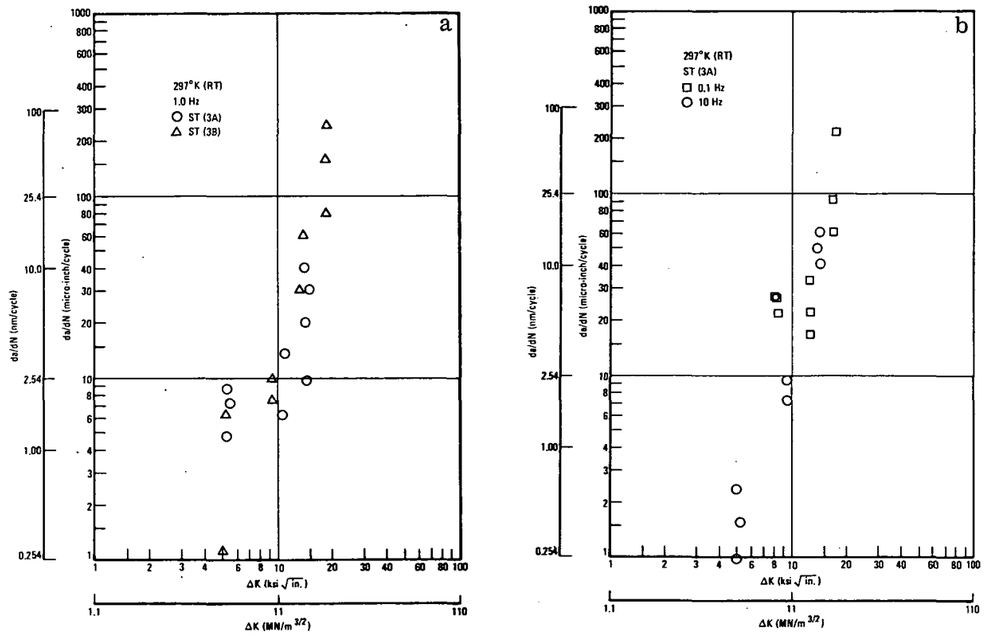

Figure 14. DCB Cyclic Flow Growth, Short Transverse

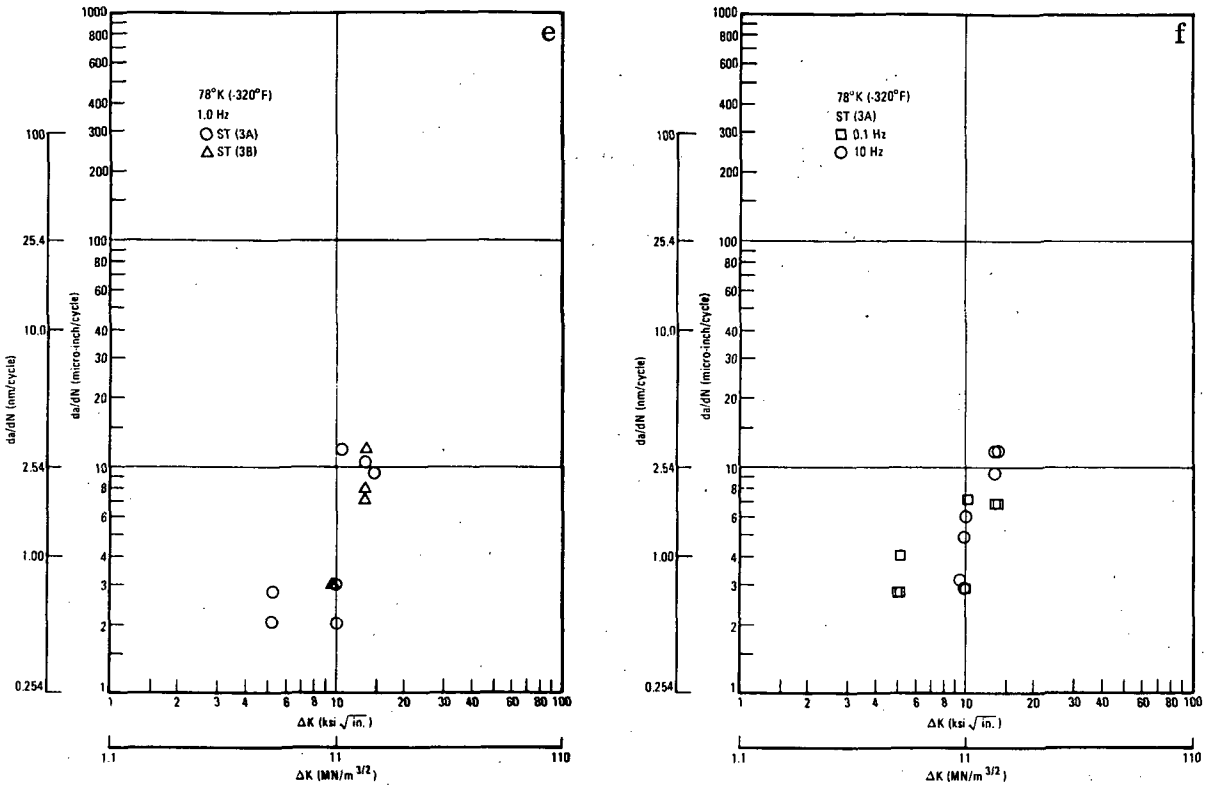

Figure 14. DCB Cyclic Flaw Growth, Short Transverse, Contd

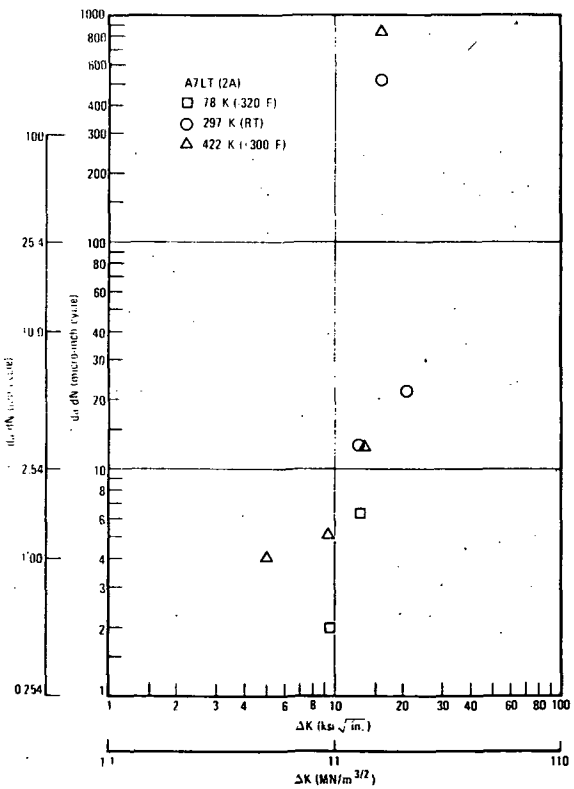

Figure 15. DCB Cyclic Flaw Growth, Long Transverse

to determine the boundaries of crack growth for a given ΔK, which made the da/dN values for that step and the next step useless.

The study indicated that the fractured surface of specimens tested at 78°K (-320° F) is harder to analyze than the surfaces of specimens tested at other temperatures. Figure 14 provides a display of the variation of crack growth rates with ΔK for the ST(3A) and ST(3B) specimens at the three test temperatures, while Figure 15 is a similar plot for the LT(2A) specimens at all three test temperatures.

The curves on the log/log scale for ST(3A) and (3B) specimens are reasonable at room temperature and 422°K (300° F). However, the crack growth for tests at 78°K (-320° F) seems to be stunted at ΔK

values greater than 11.0 $MN/m^{3/2}$ (10 ksi $\sqrt{in.}$). In general, the values obtained at the lower ΔK seem to be more erratic than those at higher ΔK. This effect is partly due to the relative spread in the logarythmic plots.

The stress ratio (R) used for this test program was 0.3, which somewhat limited the maximum ΔK available for cyclic testing. For example, assume $K_{Ic} = 30$ $MN/m^{3/2}$ and $K_{Ic} = K_{max}$ and:

$$\Delta K = K_{max} (1-R)$$

$$\Delta K = 30 (1-3)$$

$$\Delta K = 21 \text{ } MN/m^{3/2}$$

For this condition then, any crack growth at a ΔK of 21 $MN/m^{3/2}$ would cause the specimen to fail. As stated earlier, all specimens that survived cyclic testing were statically tested to failure in their respective environments.

3.2.4 DOUBLE CANTILEVER BEAM (DCB) SUSTAINED LOAD TESTS. Sustained load tests were performed on the 2.54 cm (1.0 in.) DCB specimens at room temperature (50-percent relative humidity), in 3.5-percent NaCl solution, in air at 422°K (300°F), in gaseous hydrogen at room temperature, in gaseous hydrogen at 422°K, and in liquid hydrogen. (The gaseous hydrogen tests were under a static pressure of 20 psig.)

Except for several specimen orientations (primarily L(1A)) where unorthodox failures occurred (see cyclic testing), all specimens were subjected to increasing load steps in a similar manner to the cyclic tests. Between sustained load steps, specimens were returned to a pre-cracking regimen (room temperature) to minimize crack blunting for the next load step and to prove masker bands. Ideally, the first load steps would show no crack growth, the second step would provide growth within the allotted time, and the third step would cause failure or additional crack growth. If the specimen survived the sustained load testing, it was statically tested to failure in its respective environment.

The majority of specimens were subjected to three or four load steps. Instrumentation was attached to indicate the presence of cracking and to determine if crack growth occurred upon loading. If crack growth was indicated by instrumentation, this information was noted during fractographic examination in an attempt to determine crack growth rates. As in the cyclic test specimens, crack growth was extremely difficult to determine using polarized light fractographic techniques.

Although the basic procedures were similar for all sustained load tests, these were divided into two groups: 1) hydrogen tests and 2) air and 3.5-percent NaCl solution tests. Each specimen was planned for 300 minutes of exposure at each load step.

Table 8. Sustained Load Tests of 2.54 cm (1.0 in.) DCB at Room Temperature (50 Percent Relative Humidity)

Specimen ID	Applied K_1 average		$\frac{\Delta a}{\Delta t}$		Time	Applied K_2 average		$\frac{\Delta a}{\Delta t}$		Time	Applied K_3 average		$\frac{\Delta a}{\Delta t}$		Time	Applied K_4 average		$\frac{\Delta a}{\Delta t}$		Time
	(ksi $\sqrt{in}$)	MN/$m^{3/2}$	(in/hr)	(cm/hr)	(hours)	(ksi $\sqrt{in}$)	(MN/$m^{3/2}$)	(in/hr)	(cm/hr)	(hours)	(ksi $\sqrt{in}$)	(MN/$m^{3/2}$)	(in/hr)	(cm/hr)	(hours)	(ksi $\sqrt{in}$)	MN/$m^{3/2}$	(in/hr)	(cm/hr)	(hours)
A1 L(1A)1	31.7	34.8	Vertical crack		22.3	Failed During Notch Sharpening														
A1 L(1A)2	31.8	34.9	Vertical crack		22.3	Static Tested to Failure														
A3 L(1B)1	29.1	32.0	0	0	70.5	37.0	40.7	.00306	.00777	22.9	37.3	41.0			FOL					
A7 LT(2A)2	28.7	31.5	.000444	.00113	22.5	37.4	41.1			16.5(F)										
A5 LT(2B)7	Failed During Precracking																			
A5 LT(2B)8	28.9	31.8	Vertical crack		22.5	31.7	34.8			16.5	32.6	35.8			FOL					
A11 ST(3A)4	23.2	25.5	0	0	66.25	27.6	30.3			93.5										
A11 ST(3A)5	24.0	26.4	0	0	66.25	26.9	29.6			FOL										
A11 ST(3A)6	23.4	25.7	0	0	22.5	27.5	30.2			FOL										
A9 ST(3B)4	21.3	23.4	0	0	64.7	24.3	26.7	0	0	20.9	25.5	28.0	0	0	71.6	26.8	29.4	0	0	23.7
A9 ST(3B)5	23.3	25.6	0	0	20.5	25.2	27.7	.000899	.00228	22.3	28.7	31.5			FOL					
A9 ST(3B)6	23.0	25.3	0	0	22.5	25.9	28.5	.00448	.0114	6.7	28.0	30.8			FOL					

F = failed

FOL = failed on loading

This plan was followed for hydrogen tests (most average 360 minutes), but the times were extended to 1200 minutes for the non-hydrogen tests to obtain more definitive crack growth information. It may have been advantageous to extend the hydrogen tests in a similar manner, but the expense of extending hydrogen testing beyond a one-shift operation was outside the scope of this program.

Because of the hazardous nature of gaseous and liquid hydrogen testing, the test chambers were located at the remote Sycamore Canyon test site without visual observation of the specimens during testing. Load controls and remote recording of test data was accomplished in a concrete block house about 100 feet from the test chamber. Results of the sustained load tests are shown in Tables 8 through 13.

As for the cyclic tests, the applied K values shown are average (where crack growth occurred). Crack growth rates are then shown for each load step across the table. When fracture occurred within one minute of achieving maximum load, the designation FOL (fractured on loading) was used. Where a specimen fractured after a significant amount of time, the designation F (fractured) is used following the time of exposure.

Specimens usually survived their exposure steps without noticeable flaw growth. In a few cases such as ST(3A) and (3B), specimens in gaseous hydrogen at 422°K, the tests provided optimum results: no crack growth occurred at the first load step (except for ST(3B) 19). Crack growth was observed at the second or third step, and fracture occurred during the final step. With Specimen ST(3B) 19, increasingly greater crack growth rates were observed as the applied K was increased. Similar good results were obtained at 422°K in air for the ST(3A) and (3B) specimens.

Although some results were obtained from tests in 3.5-percent NaCl solution, the crack paths were quite distorted due to the corrosive influence of the environment on subsequent load steps. Attempts to examine the fractured surfaces of these specimens with an electron microscope were also frustrated by the influence of the NaCl solution on both the sustained load growth and the cyclic marker bands.

The most difficult tests were expected to be those in liquid hydrogen, where fracture without flaw growth was expected. Half of the ST(3A) and (3B) specimens, however, provided some flaw growth readings, although the da/dt values demonstrated large scatter.

Oddly, the tests at room temperature (air or hydrogen) did not provide as much data as tests at other temperatures. In air, no single specimen provided more than one flaw growth data point. (This was not a requirement of the program, but consecutive flaw growth data points tend to lend confidence to the data.)

Table 9. Sustained Load Tests of 2.54 cm (1.0 in.) DCB at 422°K (300°F), in Air

Specimen ID	Applied K_1 average		$\frac{\Delta a}{\Delta t}$		Time	Applied K_2 average		$\frac{\Delta a}{\Delta t}$		Time	Applied K_3 average		$\frac{\Delta a}{\Delta t}$		Time	Applied K_4 average		$\frac{\Delta a}{\Delta t}$		Time
	(ksi $\sqrt{in}$)	$MN/m^{3/2}$	(in/hr)	(cm/hr)	(hours)	(ksi $\sqrt{in}$)	($MN/m^{3/2}$)	(in/hr)	(cm/hr)	(hours)	(ksi $\sqrt{in}$)	($MN/m^{3/2}$)	(in/hr)	(cm/hr)	(hours)	(ksi $\sqrt{in}$)	$MN/m^{3/2}$	(in/hr)	(cm/hr)	(hours)
A3 L(1B)3	18.0	19.8	(Vertical crack)		24.0	21.4	23.5			24.7	24.4	26.6			4.0(F)					
A7 LT(2A)4	18.4	20.2	0	0	24.0	21.7	23.8	.00206	.00523	24.3	25.3	27.8			18.8(F)					
A5 LT(2B)5	18.4	20.2	(Vertical crack)		40.0(F)															
A5 LT(2B)6	23.8	26.2	(Vertical crack)		FOL															
A11 ST(3A)16	13.1	14.4	0	0	65.0	17.1	18.8	.00310	.00787	29.0	21.1	23.2			24(F)					
A11 ST(3A)17	12.9	14.2	0	0	24.0	16.9	18.6	.00458	.0116	24.0	23.2	25.5	.0174	.0442	24.7					
A11 ST(3A)18	13.0	14.3	0	0	24.0	17.1	18.8	.00347	.00881	25.9	23.8	26.2	.0225	.0572	24.0					
A9 ST(3B)16	14.3	15.7	0	0	24.0	18.1	19.9	.00286	.00726	42.0	22.1	24.3			22.1(F)					
A9 ST(3B)17	14.4	15.8	0	0	24.0	18.4	20.2	.00240	.00610	25.0	23.8	26.2	.0108	.0274	24.1					
A9 ST(3B)18	14.4	15.8	0	0	24.0	18.8	20.7	.00194	.00493	87.5	24.0	26.4			6.3(F)					

Table 10. Sustained Load Tests of 2.54 cm (1.0 in.) DCB in 3.5 Percent NaCl

Specimen ID	Applied K_1 average		$\frac{\Delta a}{\Delta t}$		Time	Applied K_2 average		$\frac{\Delta a}{\Delta t}$		Time	Applied K_3 average		$\frac{\Delta a}{\Delta t}$		Time	Applied K_4 average		$\frac{\Delta a}{\Delta t}$		Time
	(ksi$\sqrt{in}$)	MN/m$^{3/2}$	(in/hr)	(cm/hr)	(hours)	(ksi$\sqrt{in}$)	(MN/m$^{3/2}$)	(in/hr)	(cm/Hr)	(hours)	(ksi$\sqrt{in}$)	(MN/m$^{3/2}$)	(in/hr)	(cm/hr)	(hours)	(ksi$\sqrt{in}$)	MN/m$^{3/2}$	(in/hr)	(cm/hr)	(hours)
A1 L(1B)9	29.1	32.0	0	0	22.2	35.4	38.9	.00173	.00439	17.3	38.1	41.9			FOL					
A7 LT(2A)9	23.0	25.3	0	0	18.0	28.9	31.8	0	0	21.5	33.8	37.1	0	0		37.7	41.4			FOL
A5 LT(2B)3	31.4	34.5	Vertical crack		23.7	33.6	36.9			23.7	34.4	37.8			20.0	35.7	39.2			6.75(F)
A5 LT(2B)4	26.8	29.4	Vertical crack		21.7	31.4	34.5			18.0	33.1	36.4			64.3	35.8	39.3			1.0(F)
A11 ST(3A)7	20.6	22.6	0	0	14.0	25.1	27.6	0	0	7.0	27.6	30.3	0	0	7.0	29.2	32.1			3.5(F)
A11 ST(3A)8	22.7	24.9	0	0	7.0	25.8	28.3	0	0	7.0	28.1	30.9			.75(F)					
A11 ST(3A)9	22.6	24.8	0	0	19.0	24.8	27.2	0	0	17.0	26.3	28.9	.0025	.0064	16.0	Static Test to Failure				
A9 ST(3B)7	23.8	26.2	0	0	64.0	26.5	29.1	0	0	24.0	27.6	30.3	.0104	.0264	7.0	29.3	32.2			FOL
A9 ST(3B)8	24.0	26.4	0	0	12.0	26.8	29.4	.0104	.0264	12.5	28.7	31.5			FOL					
A9 ST(3B)9	23.9	26.3	.00244	.00620	20.5	28.2	31.0	.0056	.0142	14.25	27.7	30.4			FOL					

Table 11. Sustained Load Tests of 2.54 cm (1.0 in.) DCB at Room Temperature in Gaseous Hydrogen

Specimen ID	Applied K_1 average		$\frac{\Delta a}{\Delta t}$		Time	Applied K_2 average		$\frac{\Delta a}{\Delta t}$		Time	Applied K_3 average		$\frac{\Delta a}{\Delta t}$		Time	Applied K_4 average		$\frac{\Delta a}{\Delta t}$		Time
	(ksi $\sqrt{in}$)	MN/m$^{3/2}$	(in/hr)	(cm/hr)	(hours)	(ksi $\sqrt{in}$)	(MN/m$^{3/2}$)	(in/hr)	(cm/hr)	(hours)	(ksi $\sqrt{in}$)	(MN/m$^{3/2}$)	(in/hr)	(cm/hr)	(hours)	(ksi $\sqrt{in}$)	MN/m$^{3/2}$	(in/hr)	(cm/hr)	(hours)
A1 L(1A)7	22.0	24.2	Vertical cracks		5.0	24.7	27.1	—	—	6.25	37.1	40.8	—	—	FOL					
A1 L(1A)8	19.8	21.8	—	—	6.0	24.3	26.7	—	—	6.0	34.2	37.6	—	—	5.7	36.0	39.6	—	—	FOL
A3 L(1B)4	35.7	39.2			4.0(F)															
A7 LT(2A)12	19.9	21.9	0	0	6.1	36.0	39.6	.080	.203	1.0(F)										
A5 LT(2B)1	37.2	40.9	—		5.0	42.7	46.9	—		FOL										
A5 LT(2B)2	35.6	39.1			1.5	40.0	43.9	—		FOL										
A11 ST(3A)10	11.8	13.0	0	0	6.0	15.8	17.4	0	0	6.0	20.2	22.2	0	0	6.0	24.6	27.0			FOL
A11 ST(3A)11	16.1	17.7	0	0	6.0	20.3	22.3	0	0	6.0	23.5	25.8	.00517	.0131	5.8	25.6	28.1	—	—	3.75(F)
A11 ST(3A)12	16.0	17.6	0	0	6.0	20.7	22.7	.00182	.00462	5.5	22.7	24.9	.00167	.00424	6.0	23.3	25.6	.00833	.0212	6.0
A5 ST(3B)28	16.3	17.9	0	0	6.0	21.3	23.4	0	0	6.6	23.5	25.8	0	0	6.75	26.7	29.3	—	—	FOL
A9 ST(3B)11	13.0	14.3	0	0	6.0	16.9	18.6	0	0	6.0	25.7	28.2	0	0	6.25	27.6	30.3	0	0	6.7
A9 ST(3B)12	20.8	22.9	0	0	6.3	22.8	25.1	0	0	6.1	25.9	28.5	0	0	6.6	27.0	29.7	0	0	6.0

(F) failed

FOL failed on loading

Table 12. Sustained Load Tests of 2.54 cm (1.0 in.) DCB at 422°K (300°F) in Gaseous Hydrogen

Specimen ID	Applied K_1 average		$\frac{\Delta a}{\Delta t}$		Time	Applied K_2 average		$\frac{\Delta a}{\Delta t}$		Time	Applied K_3 average		$\frac{\Delta a}{\Delta t}$		Time	Applied K_4 average		$\frac{\Delta a}{\Delta t}$		Time
	($ksi\sqrt{in}$)	$MN/m^{3/2}$	(in/hr)	(cm/hr)	(hours)	($ksi\sqrt{in}$)	($MN/m^{3/2}$)	(in/hr)	(cm/hr)	(hours)	($ksi\sqrt{in}$)	($MN/m^{3/2}$)	(in/hr)	(cm/hr)	(hours)	($ksi\sqrt{in}$)	$MN/m^{3/2}$	(in/hr)	(cm/hr)	(hours)
A1 L(1A)11	19.9	21.9			6.0	33.5	36.8			FOL										
A1 L(1A)12	20.0	22.0			6.0	30.0	33.0			FOL										
A3 L(1B)6	19.7	21.6			5.75	29.7	32.6			5.5	38.7	42.5			FOL					
A7 LT(2A)6	29.7	32.6			0.5(F)															
A5 LT(2B)15	30.5	33.5			1.4(F)	(Vertical fracture)														
A5 LT(2B)19	31.0	34.1			FOL															
A11 ST(3A)19	16.5	18.1	0	0	6.0	20.8	22.9	0	0	4.25	24.1	26.5	.0285	.0724	1.4 (F)					
A11 ST(3A)20	16.4	18.0	0	0	5.25	20.9	23.0	.0118	.0300	6.8	25.1	27.6	.0320	.0810	2.5	24.0	26.4			20(F)
A11 ST(3A)21	16.7	18.3	0	0	6.3	21.1	23.2	0	0	6.3	25.6	28.1			1.3 F					
A9 ST(3B)19	16.4	18.0	.00167	.00424	6.0	20.9	23.0	.00469	.0119	6.4	25.4	27.9	.0450	.114	6.0	26.8	29.4			1.3(F)
A9 ST(3B)20	16.4	18.0	0	0	6.6	20.8	22.9	0	0	6.0	<24.7	<27.1			FOL					
A9 ST(3B)21	16.2	17.8	0	0	6.0	20.4	22.4	0	0	6.0	26.3	28.9			6.0	24.1	26.5	Vertical Cracks		4.2

Table 13. Sustained Load Test of 2.54 cm (1.0 in.) DCB at Liquid Hydrogen Temperature

Specimen ID	Applied K_1 (average)		$\frac{\Delta a}{\Delta t}$		Time	Applied K_2 average		$\frac{\Delta a}{\Delta t}$		Time	Applied K_3 average		$\frac{\Delta a}{\Delta t}$		Time	Applied K_4 average		$\frac{\Delta a}{\Delta t}$		Time
	($ksi\sqrt{in}$)	$MN/m^{3/2}$	(in/hr)	(cm/hr)	(hours)	($ksi\sqrt{in}$)	($MN/m^{3/2}$)	(in/hr)	(cm/hr)	(hours)	($ksi\sqrt{in}$)	($MN/m^{3/2}$)	(in/hr)	(cm/hr)	(hours)	($ksi\sqrt{in}$)	$MN/m^{3/2}$	(in/hr)	(cm/hr)	(hours)
Al L(1A)13	20.2	22.2			6.0	44.9	49.3			FOL										
Al L(1A)14	43.5	47.8	(5% intercept)			51.8	56.9 (Vertical fracture)			FOL										
A3 L(1B)7	46.4	51.0			0.83(F)															
A7 L(2A)8	44.4	48.8			FOL															
A5 LT(2B)9	47.8	52.5			6.0	50.5	55.5 (Vertical fracture)			FOL										
A5 LT (2B)10	46.7	51.3			5.0(F)		(Vertical fracture)													
A11 ST(3A)25	18.3	20.1	0	0	6.0	23.9	26.3	0	0	6.0	27.2	29.9	0	0	6.0	30.3	33.3			FOL
A11 ST(3A)26	18.1	19.9	0	0	6.25	24.6	27.0	.00151	.00384	6.6	28.1	30.9								.033(F)
A11 ST(3A)27	18.2	20.0	0	0	6.40	25.5	28.0			FOL										
A5 ST(3B)25	24.4	26.8	0	0	6.0	27.8	30.5	.00492	.0125	6.1	29.3	32.3								0.5 (F)
A5 ST(3B)26	24.5	26.9	.00166	.00422	6.0	28.3	31.1			FOL										
A5 ST(3B)27	23.9	26.3	0	0	6.0	27.7	30.4	.0117	.0297	6.0	29.0	31.9	.0236	.0599						4.25(F)

3.2.5 THRESHOLD VALUES. Crack and fracture thresholds from the sustained load data are shown in Tables 14 and 15 for each of the six environments. Thresholds are defined as the stress intensity factor below which cracking or fracture does not occur within the time limit of the program. Again, the time limits for hydrogen tests was 360 minutes, with 1200 minutes for non-hydrogen tests.

Many of the values shown in the tables were quite conservative, since there were large differences in load steps for certain specimen orientations. If, for example, a specimen survived an applied K of 15 $MN/m^{3/2}$ but failed at a K of 39 $MN/m^{3/2}$, the threshold was listed as 15. In fact, the true K may fall between those two values. All thresholds for the L(1A) specimens are conservative, since all fractures occurred in the direction of loading rather than in the desired direction. The LT(2A) values for GH_2 (room temperature and 422°K air as well as the LT(2B) value in 422°K air) are probably conservative also. It appears that the fracture thresholds for the ST(3A) and (3B) orientations are higher in 3.5 percent NaCl solution than in air at 50-percent relative humidity.

3.2.6 PLANE STRAIN FRACTURE TOUGHNESS AFTER EXPOSURE. Part of the planning of this program provided for obtaining more than one type of fracture data for each DCB fracture test specimen. As reported, the optimum exposure test would have provided flaw growth information, threshold information for sustained load tests, and toughness data under subsequent static tests. However, some specimens failed under cyclic or sustained load exposures. If the specimen survived, it was tested to failure in the environment to which it was exposed.

In all cases, an apparent fracture toughness value was calculated. (The word "apparent" is used to describe the toughness values obtained in deference to ASTM Standard E99, which does not recognize a DCB as a standard plane-strain fracture toughness test specimen.) When the specimen failed during cyclic or sustained load testing, a toughness value was calculated using the maximum load and the last crack size obtainable under fractographic examination. For comparative purposes, critical crack intensity factor (apparent K_{Ic}) and maximum fracture toughness values were both calculated for the specimens statically tested to failure.

The apparent K_{Ic} value was obtained using the 5-percent secant method described by ASTM Standard E399. Flaw sizes, critical loads, apparent fracture toughness, and maximum fracture toughness values are listed in Table 16 for cyclic test specimens and in Table 17 for sustained load specimens.

In virtually all cases, there is very little difference between the apparent fracture toughness and the maximum fracture toughness for those specimens in which both values were obtained. In some cases, the two values were identical, indicating a minimum of deviation from linearity in the load-compliance curves. For hydrogen tests, only maximum fracture toughness values were calculated, since the static fracture test load-compliance curves either showed little deviation from linearity or were subjected

Table 14. Sustained Load Thresholds for 2219-T87 Aluminum (6 hour limit)

Environment	Grain Orientation	Crack Threshold ($MN/m^{3/2}$)	Crack Threshold (ksi $\sqrt{in.}$)	Fracture Threshold ($MN/m^{3/2}$)	Fracture Threshold (ksi $\sqrt{in.}$)
GH_2 (RT)	L(1A)	-	-	37.6	34.2
	LT(2A)	-	-	21.9	19.9
	LT(2B)	-	-	40.9	37.2
	ST(3A)	22.3	20.3	25.6	23.3
	ST(3B)	28.5	25.9	28.5	25.9
GH_2	L(1A)	-	-	22.0	20.0
422°K (300°F)	L(1B)	-	-	32.6	29.7
	ST(3A)	18.3	16.7	22.9	20.8
	ST(3B)	17.8	16.2	23.0	20.9
LH_2	ST(3A)	26.3	23.9	27.0	24.6
	ST(3B)	26.8	24.4	30.5	27.8

Table 15. Sustained Load Thresholds for 2219-T87 Aluminum (20 hour limit)

Environment	Grain Orientation	Crack Threshold ($MN/m^{3/2}$)	Crack Threshold (ksi $\sqrt{in.}$)	Fracture Threshold ($MN/m^{3/2}$)	Fracture Threshold (ksi $\sqrt{in.}$)
R.T., 50%	L(1A)	-	-	34.9	31.8
relative humidity	L(1B)	32.0	29.1	40.7	37.0
	LT(2A)	-	-	31.5	28.7
	LT(2B)	-	-	31.8	28.9
	ST(3A)	-	-	26.4	24.0
	ST(3B)	26.7	24.3	28.0	25.5
Air	L(1B)	-	-	23.5	21.4
422°K (300°F)	LT(2A)	20.2	18.4	23.8	21.7
	LT(2B)	-	-	20.2	18.4
	ST(3A)	14.4	13.1	26.2	23.8
	ST(3B)	15.8	14.4	20.7	18.8
3.5% NaCl	L(1B)	32.0	29.1	38.9	35.4
	LT(2A)	-	-	37.1	33.8
	LT(2B)	-	-	37.8	34.4
	ST(3A)	-	-	27.2	24.8
	ST(3B)	26.2	23.8	29.1	26.5

Table 16. Apparent Plane-Strain Fracture Toughness After Cyclic Exposure, 2.54 cm (1.0 in.) DCB

Specimen Identification	Exposure Frequency (Hz)	Critical Flaw Size (cm)	Critical Flaw Size (in.)	Critical Load (MN)	Critical Load (K)	Apparent Fracture Toughness ($MN/m^{3/2}$)	Apparent Fracture Toughness (ksi $\sqrt{in.}$)	Max K ($MN/m^{3/2}$)	Max K (ksi $\sqrt{in.}$)
297°K (75° F)									
A1 L(1A)3	1.0	2.92	1.15		3.76		35.3*		
A3 L(1B)2		3.56	1.40	0.0158	3.68	43.2	39.3	45.8	41.7
A7 LT(2A)1	1.0	2.97	1.17	0.0169	3.80	39.3	35.8	41.1	37.4
A5 LT(2B)17	1.0	2.8	1.1	0.0153	3.45	34.3	31.2*	34.8	31.7*
A5 LT(2B)18	1.0	2.8	1.1	0.0156	3.50	34.8	31.7*	34.8	31.7*
A11 ST(3A)1	1.0	4.83	1.90	0.0087	1.95	28.8	26.2	31.6	32.3
A11 ST(3A)2	1.0	3.48	1.37	0.0130	2.93	33.8	30.8	30.9	28.1
A11 ST(3A)3	1.0	3.40	1.34	0.0121	2.72		-		
A9 ST(3B)1	1.0	4.55	1.79	0.0105	2.35		-	33.2	30.2
A9 ST(3B)2	1.0	3.33	1.31	0.0129	2.90	32.5	29.6	32.7	29.8
A9 ST(3B)3	1.0	3.40	1.34	0.0125	2.80	31.9	29.0	32.3	29.4
A11 ST(3A)7	0.1	3.28	1.29	0.0121	2.71	30.0	27.3	30.0	27.3
A11 ST(3A)9	0.1	3.66	1.44	0.0128	2.87			34.4	31.3
A11 ST(3A)12	0.1	3.20	1.26	0.0128	2.87			31.3	28.5
A11 ST(3A)13	10.0	3.25	1.28	0.0121	2.71	29.9	27.2	29.9	27.2
A11 ST(3A)15	10.0	3.25	1.28	0.0121	2.72			30.0	27.3
A11 ST(3A)16	10.0	3.25	1.28	0.0121	2.72			30.0	27.3
422°K (300° F)									
A1 L(1A)9	1.0	3.05	1.20	0.0120	2.70	28.5	25.9*	29.5	25.9*
A1 L(1A)10	1.0	2.8	1.1	0.0089	2.00			19.9	18.1*
A3 L(1B)5	1.0	3.33	1.31	0.0089	2.00		-	22.4	20.4
A7 LT(2A)11	1.0	3.12	1.23	0.0144	3.24	34.7	31.6	36.7	33.4
A5 LT(2B)13	1.0	2.92	1.15	0.0089	2.00		-	20.4	18.6*
A5 LT(2B)14	1.0	3.05	1.20	0.0104	2.33	24.5	22.3*	24.5	22.3*
A11 ST(3A)13	1.0	3.51	1.38	0.0107	2.40		-	27.9	25.4
A11 ST(3A)14	1.0	3.38	1.33	0.0107	2.40	27.1	24.7	27.1	24.7
A11 ST(3A)15	1.0	3.40	1.34	0.0107	2.40			27.2	24.8
A9 ST(3B)13	1.0	3.15	1.24	0.0124	2.79	30.1	27.4	30.1	27.4
A9 ST(3B)14	1.0	3.12	1.23	0.0119	2.67	28.6	26.0	28.6	26.0
A9 ST(3B)15	1.0	3.25	1.28	0.0111	2.50	27.6	25.1	28.0	25.6
A11 ST(3A)1	0.1	3.12	1.23	0.0141	3.14		32.2	35.4	32.2
A11 ST(3A)2	0.1	2.97	1.17	0.0107	2.40			24.8	22.6
A11 ST(3A)10	0.1	3.28	1.29	0.0128	2.87			31.8	28.9
A11 ST(3A)3	10.0	3.12	1.23	0.0114	2.56	27.5	25.0	27.5	25.0
A11 ST(3A)4	10.0	3.12	1.23	0.0121	2.72			29.1	26.5
A11 ST(3A)5	10.0	3.43	1.35	0.0121	2.72			31.1	28.3
78°K (-320° F)									
A1 L(1A)15	1.0	2.8	1.1	0.0191	4.30	42.7	38.9*	45.1	41.6
A1 L(1A)16	1.0	2.8	1.1	0.0205	4.60	45.7	41.6*	46.7	42.5
A3 L(1B)8	1.0	3.00	1.18	0.0121	2.72			28.3	25.8
A3 LT(2A)7	1.0	3.10	1.22	0.0121	2.72			29.0	26.4
A5 LT(2B)11	1.0	2.8	1.1	0.0185	4.15	41.3	37.6*	41.3	37.6
A5 LT(2B)12	1.0	2.84	1.12	0.0035	0.79			Failed on loading.	
A11 ST(3A)22	1.0	3.30	1.30	0.0121	2.72			30.3	27.6
A11 ST(3A)23	1.0	3.58	1.41	0.0113	2.55	30.1	27.4	30.7	27.9
A11 ST(3A)24	1.0	3.33	1.31	0.0121	2.72			30.4	27.7
A9 ST(3B)22	1.0	3.28	1.29	0.0121	2.72			30.1	27.4
A9 ST(3B)23	1.0	3.15	1.24	0.0121	2.72			29.3	26.7
A9 ST(3B)24	1.0	3.20	1.26	0.0121	2.72			29.7	27.0
A11 ST(3A)14	0.1	3.12	1.23	0.0121	2.72			29.1	26.5
A11 ST(3A)17	0.1	3.07	1.21	0.0125	2.80	29.7	27.0	30.2	27.5
A11 ST(3A)18	0.1	3.15	1.24	0.0122	2.75	29.7	27.0	30.8	28.0
A11 ST(3A)6	10.0	3.23	1.27	0.0121	2.72			29.8	27.1
A11 ST(3A)8	10.0	3.12	1.23	0.0121	2.72			29.1	26.5
A11 ST(3A)11	10.0	3.10	1.22	0.0129	2.90	30.9	28.1	31.4	28.6

* Fracture in Plane of Loading

Table 17. Apparent Plane-Strain Fracture Toughness After Sustained Load Exposure, 2.54 (1.0 in.) DCB

Specimen Identification	Critical Flaw Size (cm)	(in.)	Critical Load (MV)	(K)	Apparent Fracture Toughness ($MN/m^{3/2}$)	(ksi $\sqrt{in.}$)	Max K ($MN/m^{3/2}$)	(ksi $\sqrt{in.}$)
297°K (75° F) in Air								
A1 L(1A)1	2.8	1.1	0.0156	3.50			Failed in precrack	
A1 L(1A)2	2.8	1.1	0.0211	4.75	47.2	43.0*	47.2	43.0
A3 L(1B)1	3.40	1.34	0.0160	3.60			41.0	37.3
A7 LT(2A)2	3.56	1.40	0.0156	3.50			41.1	37.4
A5 LT(2B)7	2.8	1.1	0.0189	4.25	42.2	38.4	Failed in preload	
A5 LT(2B)8	2.8	1.1	0.0161	3.60			35.8	32.6*
A11 ST(3A)4	3.53	1.39	0.0116	2.60			30.3	27.6
A11 ST(3A)5	3.40	1.34	0.0116	2.60			29.6	26.9
A11 ST(3A)6	3.71	1.46	0.0111	2.50			30.2	27.5
A9 ST(3B)4	4.93	1.34	0.0106	2.36	35.4	32.2	37.5	34.1
A9 ST(3B)5	3.53	1.39	0.0116	2.60			30.3	27.6
A9 ST(3B)6	3.40	1.34	0.0120	2.70			30.8	28.0
422°K (300° F) in Air								
A3 L(1B)3	3.23	1.27	0.0109	2.45			26.8	24.4
A7 LT(2A)4	3.05	1.20	0.0118	2.65			27.8	25.3
A5 LT(2B)5	2.8	1.1	0.0091	2.05			20.3	18.5†
A5 LT(2B)6	2.8	1.1	0.0118	2.65			26.4	24.0*
A11 ST(3A)16	3.51	1.38	0.0089	2.00			23.2	21.1
A11 ST(3A)17	3.43	1.35	0.0096	2.16	24.7	22.5	24.7	22.5
A11 ST(3A)18	3.43	1.35	0.0096	2.15	24.6	22.4	24.6	22.4
A9 ST(3B)16	3.38	1.33	0.0096	2.15			24.3	22.1
A9 ST(3B)17	3.40	1.34	0.0105	2.37	26.9	24.5	26.9	24.5
A9 ST(3B)18	3.78	1.49	0.0096	2.15		-	26.4	24.0
297°K (RT) in 3.5% NaCl								
A3 L(1B)9	3.51	1.38	0.0160	3.60		-	41.9	38.1*
A7 LT(2A)9	3.61	1.42	0.0156	3.50			41.4	37.7
A5 LT(2B)3	2.8	1.1	0.0178	4.00			39.8	36.2*
A11 ST(3A)4	2.8	1.1	0.0178	4.00			39.8	36.2
A11 ST(3A)7	3.25	1.28	0.0129	2.90		-	32.0	29.1
A11 ST(3A)8	3.28	1.29	0.0124	2.80		-	31.2	28.4
A11 ST(3A)9	2.92	1.15	0.0125	2.82	29.0	26.4	29.8	27.1
A9 ST(3B)7	3.45	1.36	0.0125	2.80		-	32.2	29.3
A9 ST(3B)8	3.53	1.39	0.0120	2.70		-	31.5	28.7
A9 ST(3B)9	3.78	1.49	0.0110	2.48		-	30.4	27.7
297°K (75° F) in GH_2								
A1 L(1A)7	2.8	1.1						
A1 L(1A)8	2.8	1.1	0.0178	4.00			39.8	36.2*
A3 L(1B)4	3.07	1.21	0.0185	4.15			43.9	40.0
A7 LT(2A)12	3.15	1.24	0.0167	3.75			40.4	36.8
A5 LT(2B)1	2.72	1.07	0.0216	4.85			47.4	43.1*
A5 LT(2B)2	2.77	1.09	0.0198	4.45			43.9	40.0
A11 ST(3A)10	3.99	1.57	0.0094	2.12			27.0	24.6
A11 ST(3A)11	3.63	1.43	0.0105	2.35			28.0	25.5
A11 ST(3A)12	4.27	1.68	0.0087	1.95			26.2	23.8
A5 ST(3B)28	3.35	1.32	0.0116	2.60			29.2	26.6
A5 ST(3B)11	3.81	1.50	0.0111	2.50			30.9	28.1
A5 ST(3B)12	3.23	1.27	0.0124	2.80			30.7	27.9
422°K (300° F) in GH_2								
A1 L(1A)11	2.8	1.1	0.0165	3.70			36.8	33.5*
A1 L(1A)12	2.8	1.1	0.0148	3.33			33.1	30.1*
A3 L(1B)6	2.77	1.09	0.0191	4.30			42.5	38.7
A7 LT(2A)6	2.77	1.09	0.0147	3.30			32.6	29.7
A5 LT(2B)15	2.8	1.1	0.0151	3.40			33.8	30.8*
A5 LT(2B)19	2.8	1.1	0.0149	3.35			33.3	30.3*
A11 ST(3A)19	4.11	1.62	0.0101	2.25			29.4	26.8
A11 ST(3A)20	3.00	1.18	0.0107	2.40			25.1	22.8
A11 ST(3A)21	3.68	1.45	0.0091	2.05			24.7	22.5
20°K (-423° F) in LH_2								
A1 L(1A)13	2.85	1.12	0.0218	4.90			49.3	44.9*
A1 L(1A)14	2.82	1.11	0.0253	5.70			57.0	51.9*
A3 L(1B)7	2.79	1.10	0.0228	5.13			51.0	46.4
A7 LT(2A)8	2.72	1.07	0.0222	5.00			48.8	44.4
A5 LT(2B)9	2.72	1.07	0.0254	5.70			55.6	50.6*
A5 LT(2B)10	2.77	1.09	0.0231	5.20			51.4	46.8*
A11 ST(3A)25	3.68	1.45	0.0127	2.85			34.3	31.2
A11 ST(3A)26	3.45	1.36	0.0120	2.70			42.1	38.3
A11 ST(3A)27	3.35	1.32	0.0125	2.80			31.5	28.7
A5 ST(3B)25	3.15	1.24	0.0133	3.00			32.3	29.4
A5 ST(3B)26	3.18	1.25	0.0133	2.98			32.1	29.2
A5 ST(3B)27	3.23	1.27	0.0133	3.00			32.9	29.9

* Fracture in Plane of Loading

to other noise indications that were impossible to isolate. (The hydrogen tests were monitored and recorded at a remote site through the use of extensive landlines, which may have had an influence on the compliance curves.)

In some cases, particularly for the L(1A) specimens, the toughness values calculated are quite conservative because all fractures were in the direction of loading rather than in the intended direction. In virtually all cases, the crack changed its direction directly after the cycling precracking. Consequently, for purposes of these calculations, the critical crack size usedwas in the region of 3.0 cm (1.18 in.).

As for the 0.318 cm (0.125 in.) thick specimens, toughness values are consistently lower for the ST(3A) and ST(3B) grain orientations. Also, minimum values for the ST(3A) and (3B) orientations always seemed to occur at room temperature after sustained load exposure. Again, the specimens exposed to the 3.5-percent NaCl solution provided higher fracture toughness values than the specimens exposed to room temperature air.

3.2.7 EFFECT OF NO PRECRACKING. To determine the effect of precracking of fracture and flaw growth of the 2219-T87 specimens, various tests were performed without the benefit of fatigue precracking. The following tests were performed:

a. Static test, 2.54 cm (1.0 in.) DCB, room temperature

b. Sustained load, 2.54 cm (1.0 in.) DCB, room temperature

c. Sustained load, 2.54 cm (1.0 in.) DCB, 3.5% NaCl

d. Cyclic load (1 cps), 2.54 cm (1.0 in.) DCB, room temperature, R = +0.3

e. Cyclic load (1 cps), 2.54 cm (1.0 in.) DCB, room temperature, R = +0.3

f. Static test, 0.318 cm (0.125 in.) fracture, 78°K (-320°F)

g. Cyclic load (1 cps), 0.318 cm (0.125 in.) fracture, room temperature

All tests were performed in the same manner as the corresponding precracked tests.

3.2.7.1 Static Test. The apparent plane strain fracture toughness of the non-precracked DCB Specimen (ST 3A) was 43.5 $MN/m^{3/2}$ (39.6 ksi $\sqrt{in.}$) at room temperature at 50-percent relative humidity. The majority of precracked specimens provided values of less than 32 $MN/m^{3/2}$ in tests at room temperature.

3.2.7.2 Sustained Load Tests. The specimens used in sustained load testing (DCB, ST(3A) orientation) were exposed significantly longer in the environment, with periodic observations for crack growth. One specimen exposed to room-temperature air at 50-percent relative humidity showed no crack growth for the following conditions.

K		Exposure Time
(MN/$m^{3/2}$)	(ksi $\sqrt{in.}$)	(hours)
23.3	21.3	138.4
24.3	22.1	100.0
25.3	23.0	114.0

The specimen was then statically loaded to failure providing a fracture toughness value of 42.5 MN/$m^{3/2}$ (38.7 ksi $\sqrt{in.}$).

Similarly, a second DCB specimen (ST(3A) was sustained-loaded in 3.5-percent NaCl solution as follows.

Average K		Exposure Time	a/ T	
(MN/$m^{3/2}$)	(ksi $\sqrt{in.}$)	(hours)	(μin/hr)	(nm/hr)
23.3	21.3	120.4	0	0
24.3	22.1	100.9	0	0
25.3	23.0	113.8	0	0
25.3	23.0	501.9	19.9	506
25.4	23.1	647.0	0	0

The specimen was static tested to failure at 40 MN/$m^{3/2}$ (36.4 ksi $\sqrt{in.}$). A great deal of time was required to cause a very small crack growth, and subsequent loading showed no further growth.

Two non-precracked DCB specimens (ST-3A) were cyclic-loaded at 1 Hz in air at a stress ratio of 0.3 with the following results.

ΔK		da/dN	
(MN/$m^{3/2}$)	(ksi$\sqrt{in.}$)	(nm/cycle)	(μin/cycle)
13.1	11.9	1040	41.0
13.3	12.1	1270	50.0

These values appear comparable to the results obtained for the precracked specimens (considering the small sampling).

3.2.7.3 Static Test, 0.318 cm (0.125 in.) Specimen ST(3A). The apparent plane stress fracture toughness at 78°K (-320° F) was 55.0 MN/$m^{3/2}$ (50.1 ksi $\sqrt{in.}$). As for the non-precracked DCB specimen test, this value was substantially higher than the similar precracked specimen tests, which did not exceed 36.5 MN/$m^{3/2}$ at that temperature for the ST(3A) specimens.

3.2.7.4 Cyclic Test, 0.318 cm (0.125 in.) Specimen ST(3A). Three load steps were applied without precracking. The specimens were tested at 1.0 Hz in air at room temperature with R = 0.3. The following results were obtained.

Average ΔK		da/dN	
($MN/m^{3/2}$)	(ksi $\sqrt{in.}$)	(nm/cycle)	(μin/cycle)
13.5	12.3	161	6.30
11.0	9.97	225	8.90
23.4	21.3	1810	714.0

Values obtained for the first two load steps of the unprecracked specimens fall within the scatter limits of the precracked specimens. However, the third load step provides a growth rate somewhat greater than that of the precracked ST(3A) specimens.

3.3 PART THROUGH CRACK (PTC) TESTS

Static PTC test results are shown in Table 18 for tests performed at room temperature and 78°K (-320°F). Very little differences are shown between longitudinal and long transverse specimens. As expected, alloy toughness increased somewhat at 78°K (-320°F).

There is no clear relationship between toughness and the crack aspect ratio (a/2C). It appears that the greater depth of crack provides slightly greater toughness, but the influence is very small and erratic. Since the back face magnification factor increases as flaw depth increases, the slight variation may be due to this mathematical influence.

If the maximum gross stress is examined, however, the influence of the flaw depth is not apparent. Similarly, there seems to be no correlation between gross stress and crack aspect ratio. It would seem that the specimen containing the largest crack would provide the lowest gross stress, but such was not the case.

3.3.1 PTC CYCLIC TESTS, 0.318 cm (0.125 in.) SPECIMENS. Part through crack (PTC) specimens 0.318 cm (0.125 in.) thick were cycled at slow rates (about 0.05 Hz) in room temperature air and in liquid nitrogen. Crack growth in the 2c direction was measured optically during testing and in the a and 2c directions after fracture. Results of the tests at room temperature and 78°K (-320°F) are shown in Table 19. In specimens of this thickness, flaw growth rates are difficult to measure because of the problems associated with measuring very small crack extensions. Consequently, it was almost impossible to measure more than one crack growth rate per specimen. Even those measurements were not precise, as evidenced by the rather large scatter in test data.

Where possible, the stress intensity factor at fracture was measured. Again, the inability to measure crack size and shape precisely resulted in sizable scatter.

Table 18. Plane-Strain Fracture Toughness for 2219-T87 Aluminum Using PTC Specimens

Specimen Identification	σ_G (MN/m^2)	σ_G (ksi)	a/2c	a/t	K (MN/m$^{3/2}$)	K (ksi $\sqrt{in.}$)
297° K (RT)						
B14 BLT	370	53	0.37	0.38	54	49
A15 BLT	340	49	0.33	0.42	56	51
B11 TLT	360	52	0.5	0.5	52	47
B1 TL	390	57	0.45	0.45	57	52
B3 BL	360	52	0.4	0.4	53	48
B3 TL	350	51	0.31	0.38	51	46
78° K (-320° F)						
A15 T-LT	420	61	0.38	0.38	62	56
A16 B-LT	430	62	0.43	0.43	67	61
B12 B-LT	390	56	0.35	0.35	55	50
B1 B-L	430	62	0.33	0.35	62	56
B2 T-L	410	60	0.44	0.45	62	56
B2 B-L	410	60	0.4	0.4	59	54

3.3.2 PTC CYCLIC TESTS, 2.54 cm (1.0 in.) SPECIMENS. Results of cyclic tests of the 2.54 cm (1.0 in.) thick PTC specimens are shown in Table 20. At the conclusion of each cyclic test, the specimens were statically tested to failure (except for the room temperature specimen A15 B LT). This specimen failed in the loading pin hole region during fatigue cycling, probably due to an internal defect found in the pin hole region.

Plane-strain fracture toughness values were determined at the same temperature at which the specimens were cycled (except for A18 B LT, which was cycled in liquid nitrogen and statically tested in room temperature air).

Fracture surfaces of all specimens were examined under polarized light using a stereo microscope to determine crack growth (a) values. Generally, the fracture surfaces were the most erratic that have been observed for 2219 aluminum alloy. Although continuous surface crack measurements (2c) were made during testing, correlation between a and 2c was very difficult. In one case, specimen A18 T LT at room temperature, the surface flaw propagated to a length of more than 6.35 cm (2.50 in.) although the crack depth never exceeded 1.27 cm (0.50 in.). However, the fractured surface revealed an uneven tongue that tapered away from the plane of the crack until it resembled a delamination-type prism. Such center-plate tongues are not uncommon, but they are usually found in static tests.

Cyclic flaw growth rates were calculated and are shown in Table 20, but there are many inconsistencies in the results.

Table 19. Cyclic Flaw Growth in 2219 Aluminum, 0.318 cm (0.125 in.) PTC Specimens, R = 0.1

Specimen Identification	Max Load (MN)	Max Load (K)	Cycles	Crack Growth (da) (cm)	Crack Growth (da) (in.)	ΔK ($MN/m^{3/2}$)	ΔK (ksi $\sqrt{in.}$)	da/dN (nm/cycle)	da/dN (μin/cycle)
297°K (75° F)									
A19 T-LT	0.0890	20.0	1950	0.094	0.037	8.03	7.31	-	-
	0.178	40.0	1414	0.094	0.037	24.9	22.7	665	26.2
	0.196	44.0	Failed on loading a_c = 0.08			36.0 K_C	32.8		
A19 B-LT	0.0890	20.0	5750			5.47	4.98		
	0.133	30.0	1490	0.178	0.070	10.6	9.64	508	20.
	0.189	42.5	Failed on loading a_c = 0.08			14.5	13.2	3810	150
						17.9	16.3	1880	74.1
						29.1 K_C	26.5		
A19 M-LT	0.133	30.0	5930	0.076	0.03	16.0	14.6	282	11.1
	0.178	40.0	62 (failed) a_c = 0.08	0.025	0.01	22.5	20.5	4090	161.
						25.2 K_C	22.9		
78°K (-320° F)									
B15 B-LT	0.178	40.0	2836	0.157	0.062	22.1	20.1	376	14.8
	0.187	42.0	Failed on loading a = 0.082 2c = 0.215			28.2 K_C	25.7		
B15 T-LT	0.0890	20.0	7600	-	None	7.98	7.26	0	0
	0.133	30.0	1019	0.033	0.013	13.8	12.6	325	12.8
	0.178	40.0	2179	0.127	0.05	27.4	24.9	582	22.9
			a_c = 0.098			31.5 K_C	28.7		
B15 M-LT	0.178	40.0	515	0.008	0.003	17.9	16.3	147	5.8
	0.178	40.0	1015	0.018	0.007	18.7	17.0	175	6.9
	0.178	40.0	1387 Failed in Bending	0.046	0.018	22.0	20.0	330	13.0

Table 20. Flaw Growth for 2.54 cm (1.0 in.) PTC Tests

Specimen Identification	a/2c	ΔK ($MN/m^{3/2}$)	ΔK (ksi $\sqrt{in.}$)	Δa/ΔN (nm/c)	Δa/ΔN (μin./c)	Cycles	K_{Ic} ($MN/m^{3/2}$)	K_{Ic} (ksi $\sqrt{in.}$)
297°K (75°F)								
B12 T LT	0.40		14.5	73.4	2.9	14,000		
							57.2	52.1
A18 T LT	0.4	7.5	6.8	0	0	3,628		
	0.4	15.4	14.0	373	14.7	2,725		
	0.4	38.6	35.2	251	9.9	3,027		
	0.25						47.4	43.2
A15 B LT	0.25	14.7	13.4	0	0	2,321		
		21.4	19.5		11.0	3,165		
78°K (-320°F)								
A18 B LT	0.33	14.6	13.3	0	0	2,725		
		27.7	25.2	279	24.9	1,205		
		28.0	25.5	210	8.3	1,205		
		30.0	27.3	693	27.3	1,100		
							66.5*	60.6*
B14 T LT	0.32	13.6	12.4	0	0	2,162		
		27.8	25.3	3350	132	912		
							67.4	61.4
B11 B LT	0.25	13.6	12.4	0	0	2,346		
		21.5	19.6	940	37.0	1,350		
		27.9	25.4	2470	97.4	719		
		29.0	26.4	1100	43.4	691		
							64.2	58.5

*Static Tested at 297°K (75°F)

3.4 STIFFENED PANEL TESTS

Stiffened panel testing consisted of static tests without precracks, precracked static tests, and cyclic tests at 1.0 Hz. The three types of tests were divided into three geometries:

Leg Thickness		Bolt Hole Diameter	
(cm)	(in.)	(cm)	(in.)
0.318	0.125	0.635	0.250
1.27	0.500	0.635	0.250
1.27	0.500	1.27	0.500

Results are shown in Tables 21, 22, and 23. Crack lengths are measured from the center of the bolt hole to the left and to the right, with the thick base of the simulated panel at the bottom. For cyclic tests, more than one crack length value is shown at its respective cycle.

A finite element program was modified to model the crack emanating from a loaded bolt hole. Using the results of the program, the crack intensity factor (K) may be determined if the value of a is known. Such calculations can be made using Figure 16.

Knowing a, f(a) is obtained from the curve. The values for a, f(a), load (P), and thickness (t) are then entered in the equation:

$$K = \frac{P}{t}\sqrt{\pi a}\ f(a)$$

The program is still under development and results from this solution should be considered preliminary. For this reason, the final K values have not been tabulated in Tables 21 through 23. These solutions should be used only for a values less than 0.5.

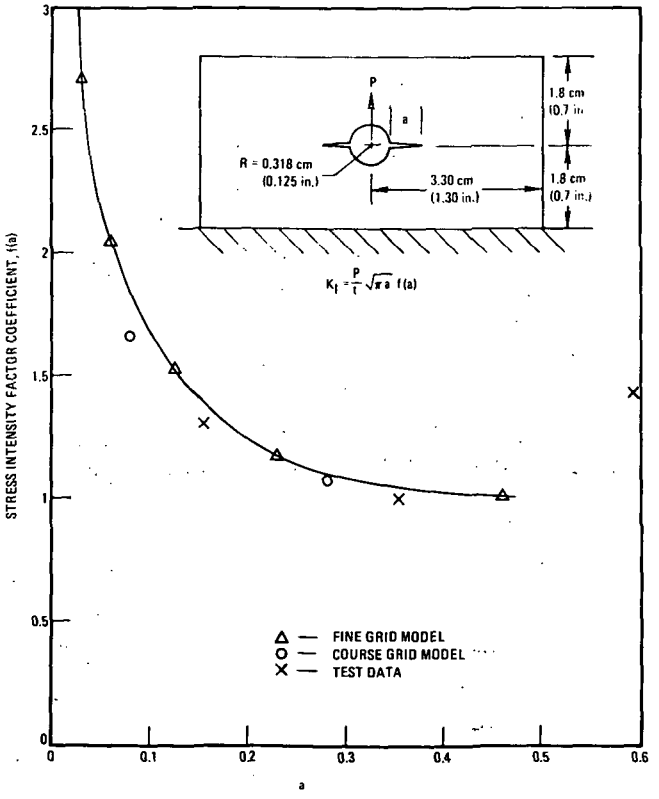

Figure 16. Cracks Emanating from a Loaded Hole

Table 21. Simulated Stiffened Panel Tests, 0.635 cm (0.250 in.) Diameter Hole in 0.318 cm (0.125 in.) Thick Leg

Specimen No.	Specimen Description	Precracking Data (R = +0.1) t* (cm)	t* (in.)	Load (kg)	Load (lb)	Cycles (× 10^3)	L. C. L. (cm)	L. C. L. (in.)	R. C. L. (cm)	R. C. L. (in.)	Test Description	Cyclic Load, R = +0.1 (kg)	(lb)	No. of Cycles	After Cyclic Test L. C. L. (cm)	L. C. L. (in.)	R. C. L. (cm)	R. C. L. (in.)	Static Load to Failure (kg)	(lb)
B18-7	Uncracked	0.327	0.1288	-	-	-	-	-	-	-	Static	-	-	-	-	-	-	-	2319	5150
B18-1	Precracked	0.309	0.1217	583	1287	100	1.130	0.445	1.079	0.425	Static	-	-	-	1.14	0.45	1.22	0.48	1740	3840
B18-5	Precracked	0.278	0.1094	583	1287	100	0.622	0.245	0.622	0.245	Static	-	-	-	0.711	0.28	0.635	0.25	1820	4010
B18-6	Precracked	0.272	0.1072	583	1287	30	0.495	0.195	0.495	0..195	Cyclic	680	1500	3,600	-	-	-	-	-	-
														7,200	0.762	0.30	0.787	0.31	NF	
B17-19	Precracked	0.331	0.1301	700	1545	50	0.825	0.325	0.698	0.275	Cyclic	1228	2700	1,624	0.762	0.30	0.686	0.27	Cyclic failure	
B18-4	Precracked	0.337	0.1336	583	1287	102	0.951	0.375	0.850	0.335	Cyclic	680	1500	3,600	1.04	0.41	0.965	0.38	NF	
														7,200	1.24	0.49	1.24	0.49		
														11,000	1.45	0.57	1.45	0.57		
B17-20	Precracked	0.334	0.1323	700	1545	60	1.205	0.475	1.079	0.425	Cyclic	680	1500	3,600	1.24	0.49	1.22	0.48	NF	
														7,200	1.39	0.55	1.32	0.52		
														10,800	1.50	0.59	1.39	0.55		
														14,400	1.730	0.68	1.80	0.71		
B18-3	Precracked	0.336	0.1328	583	1287	150	0.698	0.275	0.825	0.325	Cyclic	1228	2700	1,800	0.940	0.37	0.787	0.31	Cyclic failure	
														2,652	1.35	0.53	1.45	0.57		
B18-2	Precracked	0.336	0.1328	466	1030	80	0.368	0.145	0.368	0.215	Cyclic	1228	2700	3,600	0.432	0.17	0.686	0.27	Cyclic failure	
														5,462	0.940	0.37	1.22	0.48		

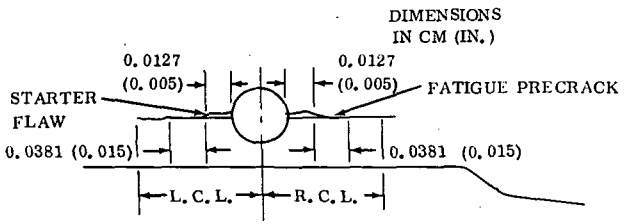

Notes:

1. K_I for 0.318 cm (0.125 in.) = 36 $MN/m^{3/2}$ (33 ksi $\sqrt{in.}$)
   K_I for 2.54 cm (1.00 in.) = 30 $MN/m^{3/2}$ (27 ksi $\sqrt{in.}$)
2. L. C. L. and R. C. L. are mostly average values for angular crack front.

* t = thickness of outstanding leg

Table 22. Simulated Stiffened Panel Tests, 0.635 cm (0.25 in.) Diameter Hole in 1.27 cm (0.50 in.) Thick Leg

Specimen No.	Specimen Description	Precracking Data (R = +0.1) t* (cm)	t* (in.)	Load (kg)	Load (lb)	Cycles (x 10^3)	L. C. L. (cm)	L. C. L. (in.)	R. C. L. (cm)	R. C. L. (in.)	Test Description	Cyclic Load, R = +0.1 (kg)	Cyclic Load, R = +0.1 (lb)	No. of Cycles	After Cyclic Test L. C. L. (cm)	After Cyclic Test L. C. L. (in.)	After Cyclic Test R. C. L. (cm)	After Cyclic Test R. C. L. (in.)	Static Load to Failure (kg)	Static Load to Failure (lb)
B17-2	Uncracked	1.29	0.5063	-	-	-	-	-	-	-	Static	-	-	-	-	-	-	-	6270	>13,850 (NF)
B17-5	Precracked	1.27	0.5003	906	2000	400	0.622	0.245	0.622	0.245	Static	-	-	-	0.762	0.30	0.711	0.28	5890 (pin failure)	>13,000 (NF)
B17-9	Precracked	1.26	0.4959	906	2000	122	0.013	<0.005	0.013	<0.005	Static	-	-	-	1.02	0.40	0.635	0.25	NF	
B17-1	Precracked	1.27	0.5011	544	1200	1001	0.419	0.165	0.521	0.205	Cyclic	3488	7700	3000 6860	0.330	0.13	0.508	0.20	NF	
B17-3	Precracked	1.28	0.5040	453	1000	1506	0.495	0.195	0.572	0.225	Cyclic	3488	7700	3000 6000 11000	0.330 0.330 0.330	0.13 0.13 0.13	0.406 0.559 0.635	0.16 0.22 0.25	NF	
B17-4	Precracked	1.25	0.4916	544	1200	1009	0.826	0.325	0.445	0.175	Cyclic	1993	4400	3600 7200 11000	0.686 0.737 0.787	0.27 0.29 0.31	0.330 0.330 0.330	0.13 0.13 0.13	NF	
B17-6	Precracked	1.28	0.5053	453	1000	6966	1.59	0.625	0.0	0.0	Cyclic	1993	4400	3600 7200 11000	0.965 0.991 1.02	0.38 0.39 0.40	0.330 0.330 0.737	0.13 0.13 0.29	NF	
B17-7	Precracked	1.29	0.5075	544	1200	2149	0.953	0.375	0.0	0.0	Cyclic	1993	4400	3600 7200 11000	0.914 0.965 0.991	0.36 0.38 0.39	0.356 0.381 0.381	0.14 0.15 0.15	NF	
B17-8	Precracked	1.29	0.5085	544	1200	1005	0.775	0.305	0.0	0.0	Cyclic	3488	7700	3000 6000 11000	0.711 0.762 0.813	0.28 0.30 0.32	0.330 0.330 0.330	0.13 0.13 0.13		

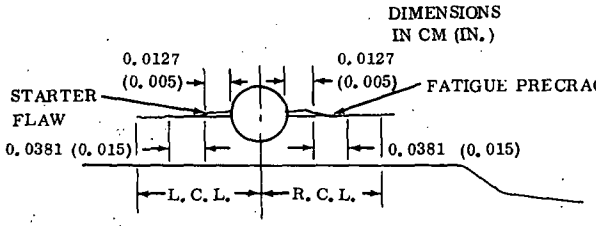

Notes:

1. K_I for 0.318 cm (0.125 in.) = 36 $MN/m^{3/2}$ (33 ksi $\sqrt{in.}$)
   K_I for 2.54 cm (1.00 in.) = 30 $MN/m^{3/2}$ (27 ksi $\sqrt{in.}$)
2. L. C. L. and R. C. L. are mostly average values for angular crack front.

* t = thickness of outstanding leg

Table 23. Simulated Stiffened Panel Tests, 1.27 cm (0.50 in.) Diameter Hole in 1.27 cm (0.50 in.) Thick Leg

Specimen No.	Specimen Description	Precracking Data (R = +0.1) t* (cm)	t* (in.)	Load (kg)	Load (lb)	Cycles ($\times 10^3$)	L. C. L. (cm)	L. C. L. (in.)	R. C. L. (cm)	R. C. L. (in.)	Test Description	Cyclic Load, R = 0.1 (kg)	(lb)	No. of Cycles	After Cyclic Test L. C. L. (cm)	L. C. L. (in.)	R. C. L. (cm)	R. C. L. (in.)	Static Load to Failure (kg)	(lb)
B17-14	Uncracked	1.28	0.5046	-	-	-	-	-	-	-	Static	-	-	-	-	-	-	-	9173	20,250
B17-16	Precracked	1.29	0.5064	1359	3000	800	1.37	0.54	1.14	0.45	Static	-	-	-	2.13	0.84	1.80	0.71	3533	7800
B17-10	Precracked	1.27	0.4990	906	2000	3528	1.46	0.575	1.33	0.525	Cyclic	1450	3200	3600	1.85	0.73	1.68	0.66	NF	
														7200	1.85	0.73	1.75	0.69		
														11000	2.06	0.81	1.83	0.72		
B17-12	Precracked	1.28	0.5024	1359	3000	236	1.10	0.435	1.31	0.515	Cyclic	2537	5600	3600	1.68	0.66	1.68	0.66	Cyclic failure	
														7200	1.91	0.75	1.83	0.72		
														7580	2.95	1.16	2.62	1.03		
B17-13	Precracked	1.28	0.5058	1359	3000	235	1.33	0.525	1.59	0.625	Cyclic	1450	3200	3600	1.68	0.66	1.73	0.68	NF	
														7200	1.68	0.66	1.83	0.72		
														11000	1.68	0.66	1.93	0.76		
B17-15	Precracked	1.28	0.5059	906	2000	1653	1.49	0.585	1.26	0.495	Cyclic	2537	5600	3600	1.60	0.63	1.45	0.57	Cyclic failure	
														5370						
B17-17	Precracked	1.29	0.5085	1359	3000	200	1.49	0.585	1.84	0.725	Cyclic	1450	3200	3600	1.65	0.65	2.01	0.79	NF	
														7200	1.80	0.71	2.03	0.80		
														11000	1.91	0.75	2.03	0.80		
B17-18	Precracked	1.30	0.5103	1359	3000	255	1.64	0.645	1.36	0.535	Cyclic	2537	5600	3600	1.63	0.64	1.79	0.70	Cyclic failure	
														4125	2.34	0.92	2.24	0.88		

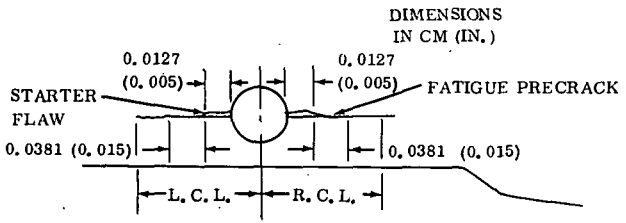

Notes:

1. K_I for 0.318 cm (0.125 in.) = 36 $MN/m^{3/2}$ (33 ksi $\sqrt{in.}$)
   K_I for 2.54 cm (1.00 in.) = 30 $MN/m^{3/2}$ (27 ksi $\sqrt{in.}$)
2. L. C. L. and R. C. L. are mostly average values for angular crack front.

* t = thickness of outstanding leg

SECTION 4

CONCLUSIONS

The material supplied for this program is somewhat unusual compared to other sheet or plate 2219-T87 aluminum alloy. Since the material was supplied in the 8.26 cm (3.25 in.) thick plate condition, it seems reasonable that such a material would require fastidious processing to provide the required mechanical properties. The microstructure, tensile test results, surface flaw test results, and some of the DCB test results suggest that this material would have different behavior than materials in thinner gages, even within the acceptable limits for plane strain.

Since no certifications of properties were obtained with the material, it is possible that the processing provided an alloy with slightly less cold work than required for T87 while providing greater toughness and slightly less strength. The toughness values obtained were similar to those of the newer 2219 alloy, known as 2419 aluminum alloy. Even so, the tested material would probably be representative of 2219-T87 (or its new designation) in plate thicknesses greater than 7.62 (3.00 in.).

The purpose of this program was to obtain data for the alloy at temperatures from 20°K (-423° F) to 422°K (300° F) in various environments and under various loading conditions. Data was obtained under static, cyclic, and sustained load conditions for six grain orientations using various types of specimens. The following general conclusions may be drawn.

a. The apparent plane-strain and plane-stress fracture toughness of 2219-T87 aluminum alloy is lowest when material is loaded in the short transverse grain direction, independent of the test temperature. When toughness values of 0.318 cm (0.125 in.) thick specimens were determined in air at 50 percent relative humidity, for example, all short transverse specimens provided values less than 45 $MN/m^{3/2}$, while values exceeding 65 $MN/m^{3/2}$ were obtained for other grain orientations. These relative numbers held for similar specimens tested in liquid nitrogen. Similarly, apparent plane strain fracture toughness values obtained from 2.54 cm (1.00 in.) thick DCB specimens were about 30 for short transverse and 37 $MN/m^{3/2}$ for longitudinal or long transverse orientations after previous cyclic exposure in room temperature air.

   While the exact ratio of toughness for longitudinal to short transverse grain directions varies somewhat, the same relative observation can be made at 422°K and 78°K for specimens exposed cyclically or to sustained loads as well as for specimens exposed cyclically or to sustained loads as well as for specimens exposed to 3.5 percent NaCl solution.

b. The apparent fracture toughness of the material is higher for specimens that are 0.318 cm (0.125 in.) thick than for specimens that are 2.54 cm (1.00 in.) thick.

In addition to the values shown in paragraph a, other results justify this conclusion. For example, the highest fracture toughness value obtained for tests of 2.54-cm-thick DCB specimens in air was 47.2 $MN/m^{3/2}$, while the maximum value for a 0.318-cm specimen was 68.1 $MN/m^{3/2}$. Again, approximately the same relative ratios were noted for other environmental conditions.

c. Apparent plane strain fracture toughness values obtained from part-through-crack specimens are higher than results obtained from other specimens.

Since static PTC test specimens were 2.54 cm thick, the results should be comparable to the DCB test results. At room temperature, the apparent plane strain fracture toughness values ranged from 51 to 57 $MN/m^{3/2}$ for PTC tests (up to 67 at 78°K), while comparable values for the DCB tests were in the low 40s.

SECTION 5

REFERENCES

1. Brown, W. F. and Srawley, J. E., Plane Strain Crack Toughness Testing of High Strength Materials, ASTM Special Publication No. 410, March 1967.

2. Brown, W. F., Review of Developments in Plane Strain Fracture Toughness Testing, ASTM STP 463, September 1970.

3. Gallagher, J. P., "Experimentally Determined Stress Intensity Factors for Several Contoured Double Cantilever Beam Specimens," Engineering Fracture Mechanics, Vol. e, 1971.

4. Mostovoy, S., Crosley, P. B., Repling, E. J., "Use of Crack Line Loaded Specimens for Measuring Plane-Strain Fracture Toughness, Journal of Materials, Vol. 2, No. 3, 1967.

5. Amateau, M. F., and Steigerwald, E. A., "Test Methods for Determining Fracture Toughness of Metallic Materials," AFML-TR-67-145, 1967.

6. Hoagland, R. G., "On the Use of the Double Cantilever Beam Specimens for Determining the Plane Strain Fracture Toughness of Metals," Journal of Basic Engineering, September 1967.

7. Hoagland, R. G., Bement, A. L., and Rowe, R. G., "Applications of Fracture Mechanics in Evaluating Initiation and Propagation of Brittle Fracture in Reactor Structural Components," Effects of Radiation on Structural Metals, ASTM STP 426, 1967.

8. Freed, C. N., "Effect of Side Grooves and Fatigue Crack Length on Plain-Strain Fracture Toughness," NRL Report 6654, 1967.

9. Freed, C. N., Goode, R. J., and Judy, R. W., Jr., "Comparison of Fracture Toughness Test Procedures for Aluminum Alloys," NRL Report 6653, 1969.

10. ASTM, ASTM Standards, Part 31, 1972.

11. Wessel, E. T., "State of the Art of the WOL Specimen for K_{Ic} Fracture Toughness Testing," Engineering Fracture Mechanics, Vol. 1, 1968.

12. Wilson, W. K., "Stress Intensity Factors for Deep Cracks in Bending and Compact Tension Specimens," Engineering Fracture Mechanics, Vol. 2, 1970.

13. Kropp, C. J., "Development of Improved Aerospace Vehicle Materials," Convair Aerospace Report GDC-ERR-AN-1210, 1967.

GENERAL DYNAMICS

Convair Aerospace Division